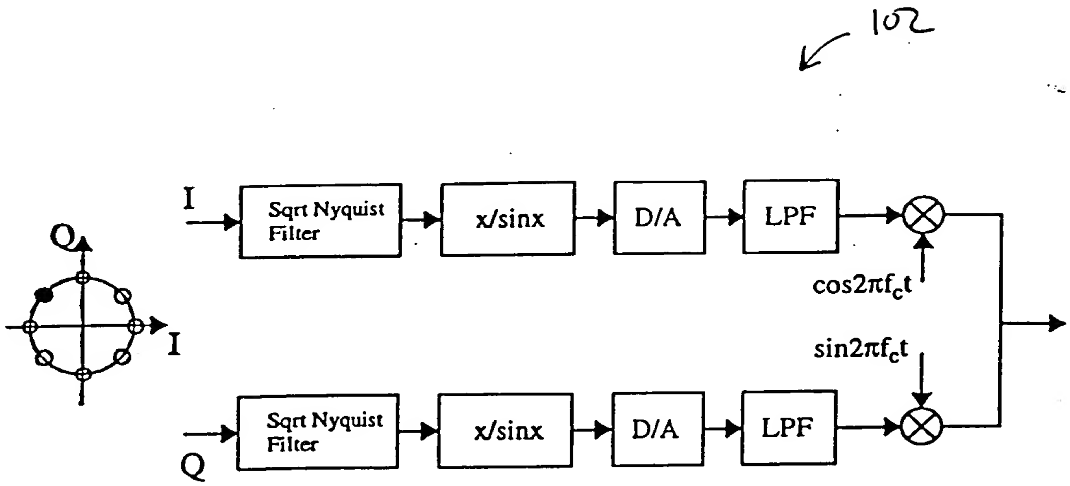

Figure 1A A simplified PSK transmitter.

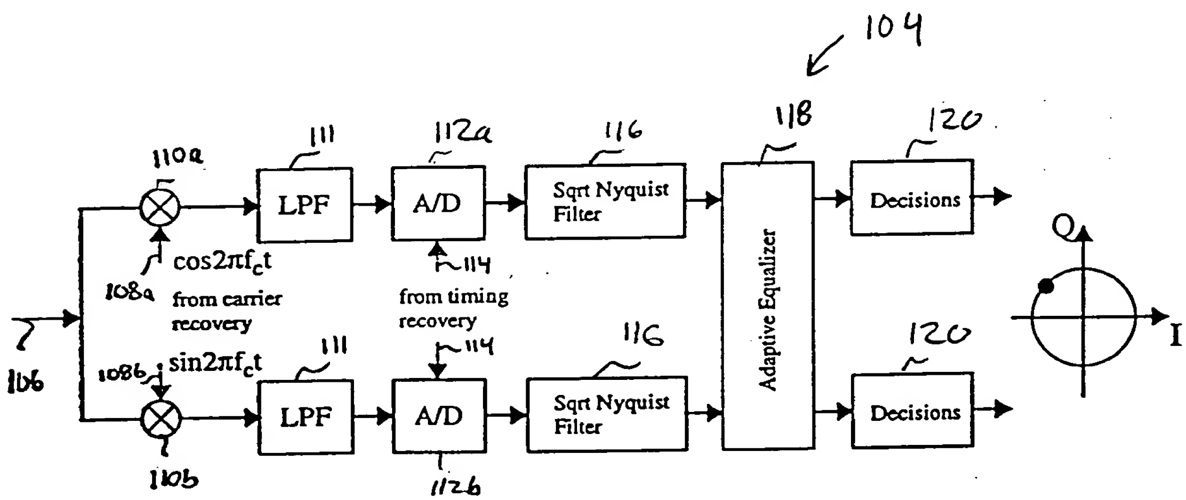

Figure 1B A simplified PSK receiver.

126

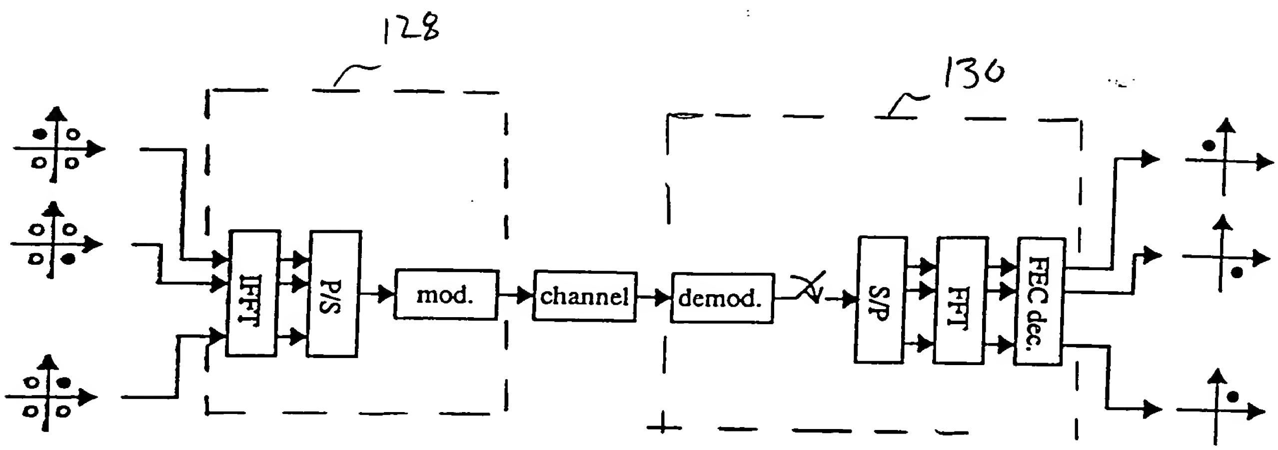

Figure 1C Simplified block diagram of an OFDM system.

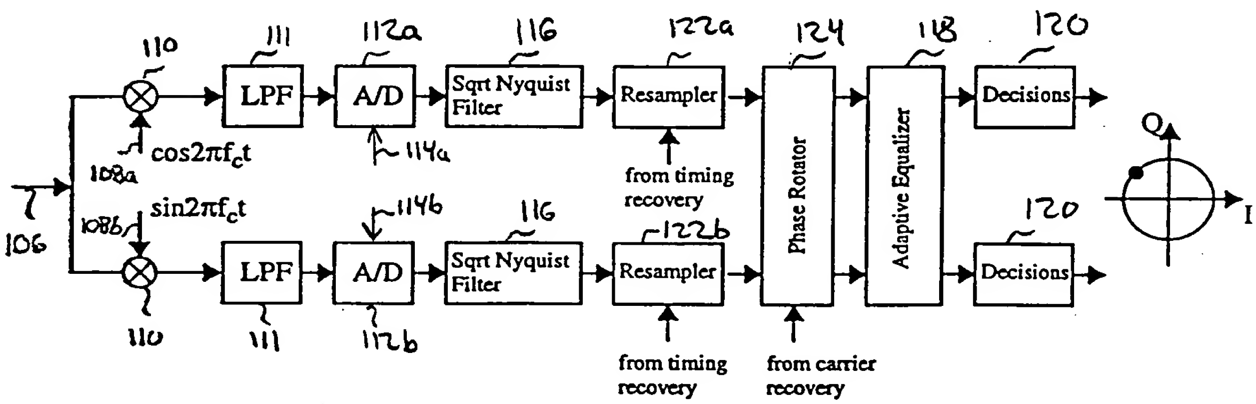

Figure 1D PSK receiver with carrier and timing recovery.

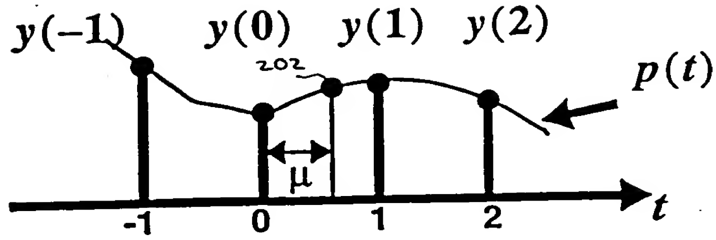

Figure 2 Interpolation Environment

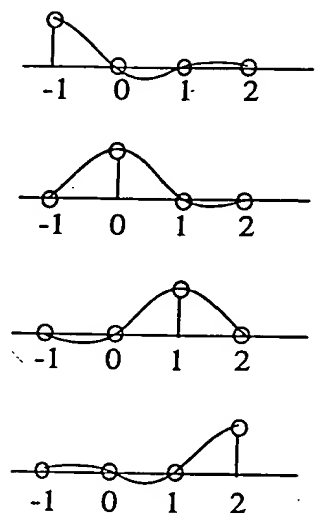

$$C_{-1}(\mu) = -\frac{1}{6}\mu^3 + \frac{1}{2}\mu^2 - \frac{1}{3}\mu$$

$$C_0(\mu) = \frac{1}{2}\mu^3 - \mu^2 - \frac{1}{2}\mu + 1$$

$$C_1(\mu) = -\frac{1}{2}\mu^3 + \frac{1}{2}\mu^2 + \mu$$

$$C_2(\mu) = \frac{1}{6}\mu^3 - \frac{1}{6}\mu$$

Figure 3 The Lagrange basis polynomials.

400

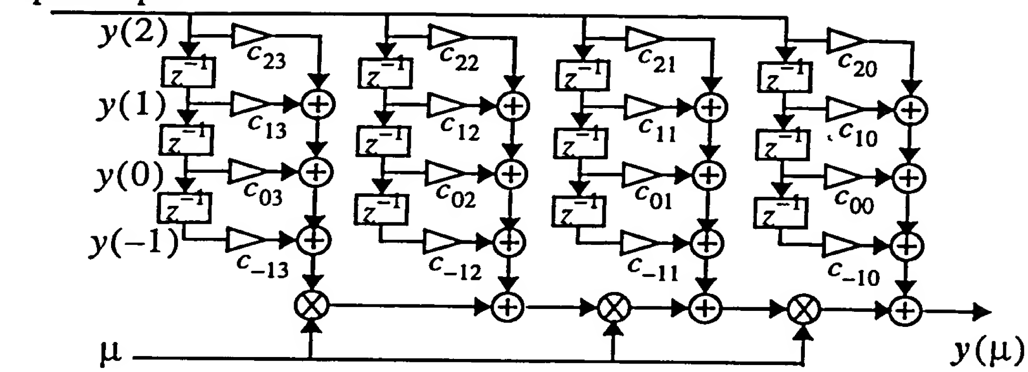

Figure 4 The Farrow structure that implements (2.5) and (2.6).

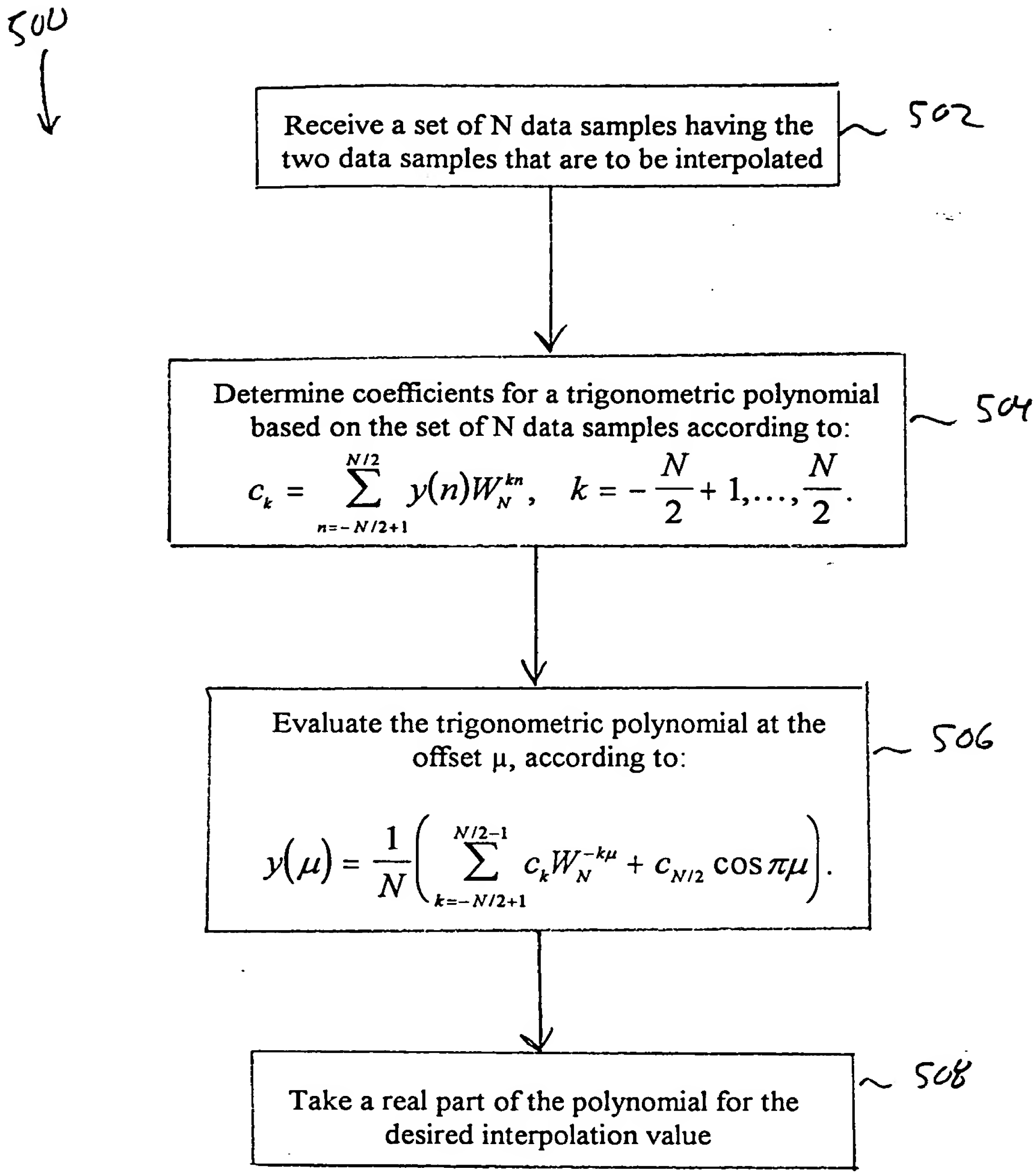
500
Receive a set of N data samples having the two data samples that are to be interpolated
502
Determine coefficients for a trigonometric polynomial based on the set of N data samples according to:
$$c_k = \sum_{n=-N/2+1}^{N/2} y(n) W_N^{kn}, \quad k = -\frac{N}{2}+1, \ldots, \frac{N}{2}.$$
504
Evaluate the trigonometric polynomial at the offset μ, according to:
$$y(\mu) = \frac{1}{N}\left(\sum_{k=-N/2+1}^{N/2-1} c_k W_N^{-k\mu} + c_{N/2} \cos \pi\mu \right).$$
506
Take a real part of the polynomial for the desired interpolation value
508

FIG. 5

FIG. 6A

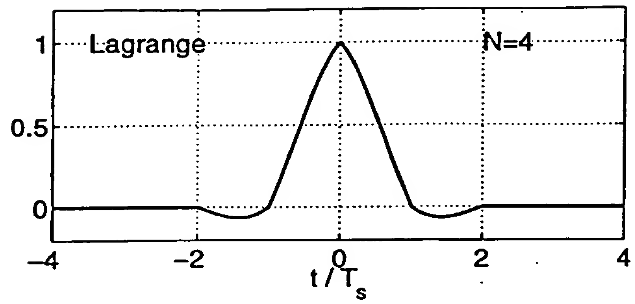

FIG. 6B

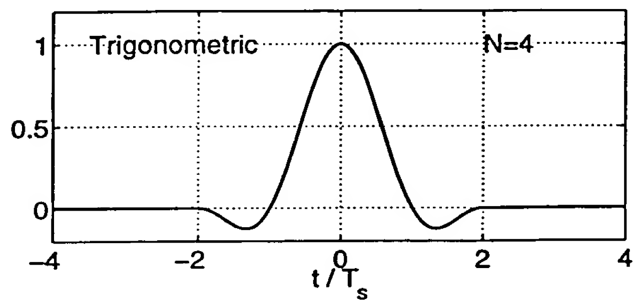

FIG. 6A-6B Impulse responses of (a) Lagrange interpolator and (b) Trigonometric interpolator.

FIG. 7A

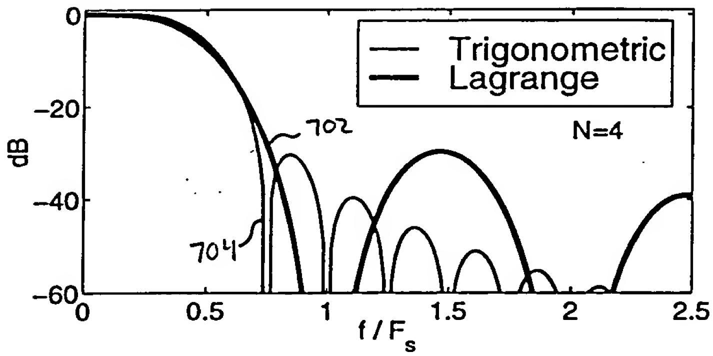

FIG. 7B

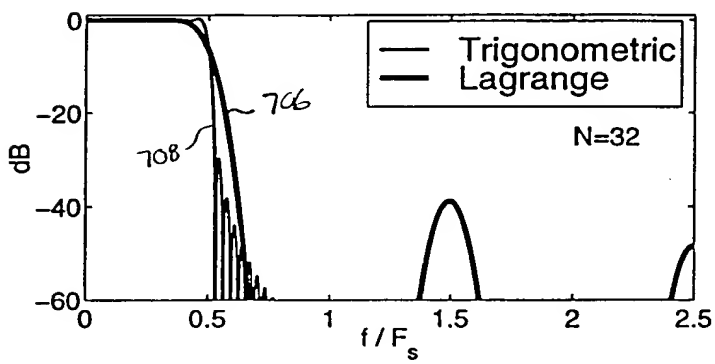

FIG. 7A-7B: Frequency responses for (a) N=4 and (b) N=32.

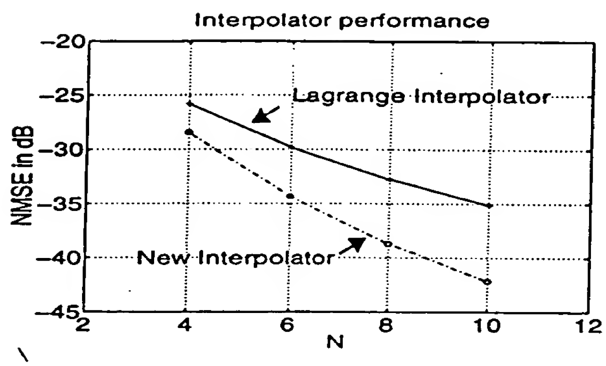

Figure 8B NMSE of the interpolated signal.

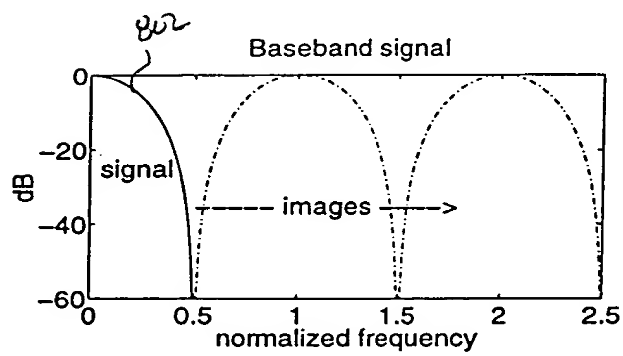

Figure 8A Signal with two samples/symbol and 100% excess BW.

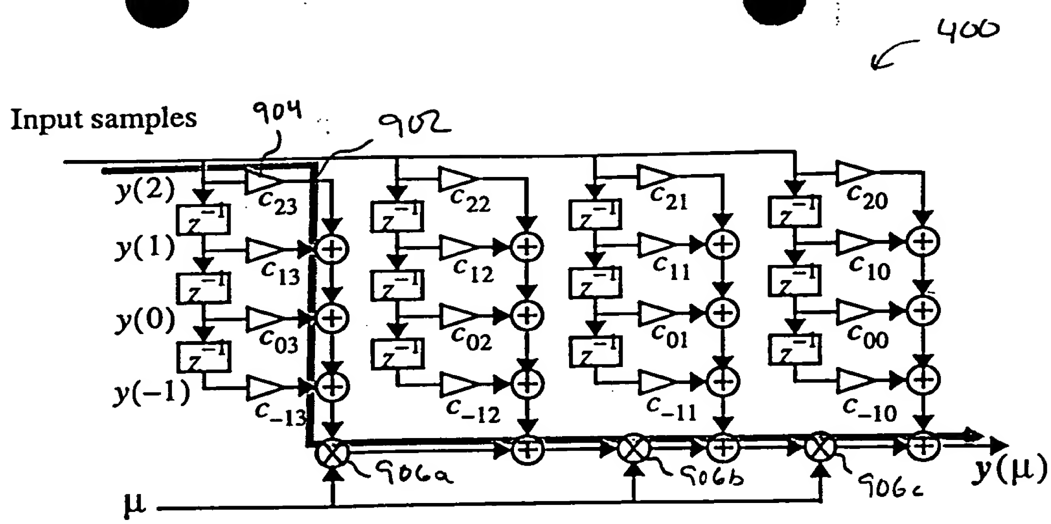

Figure 9 The critical path of the Lagrange cubic interpolator.

0003Q1 " 64289960

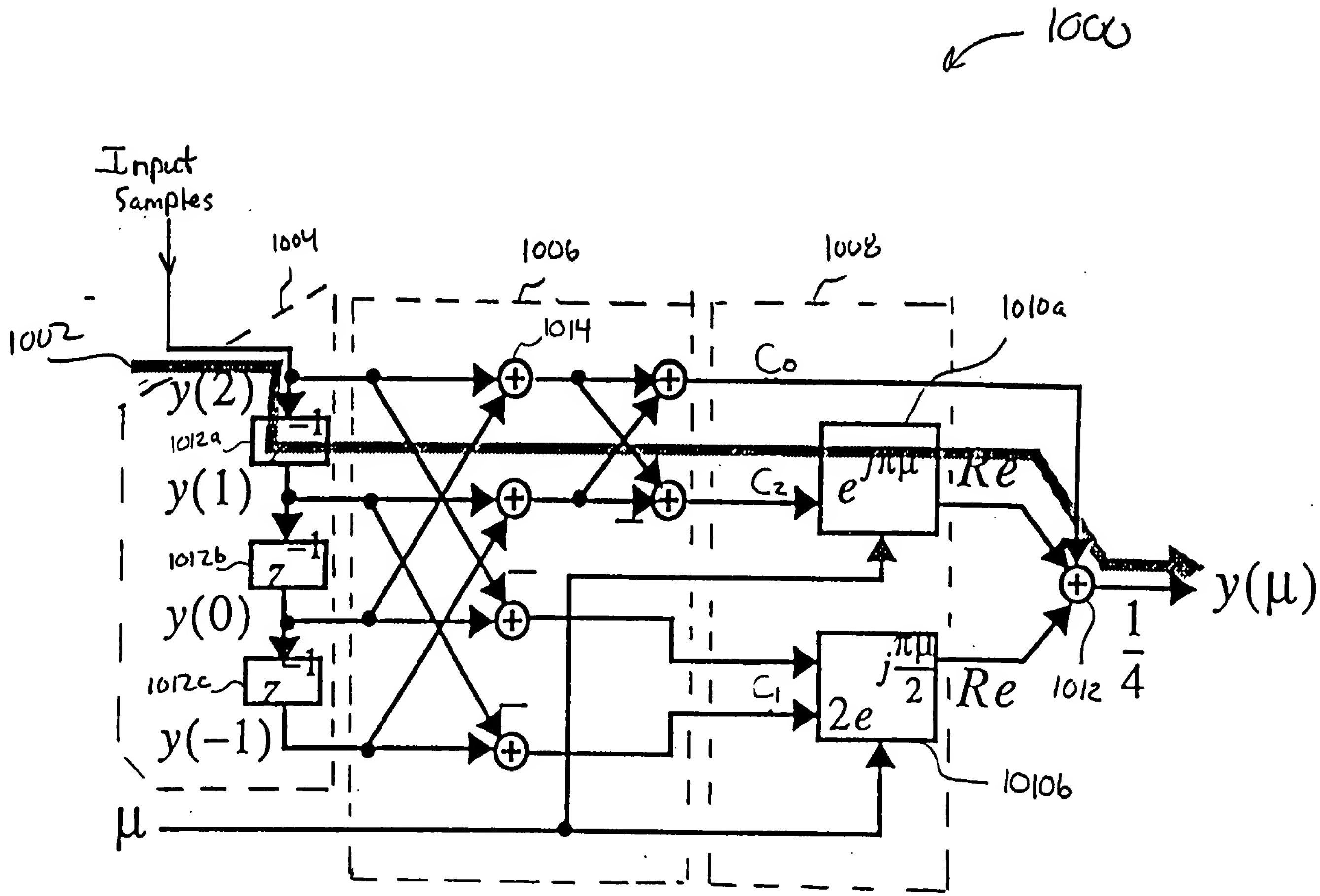

FIG. 10: Trignometric Interpolator (N=4)

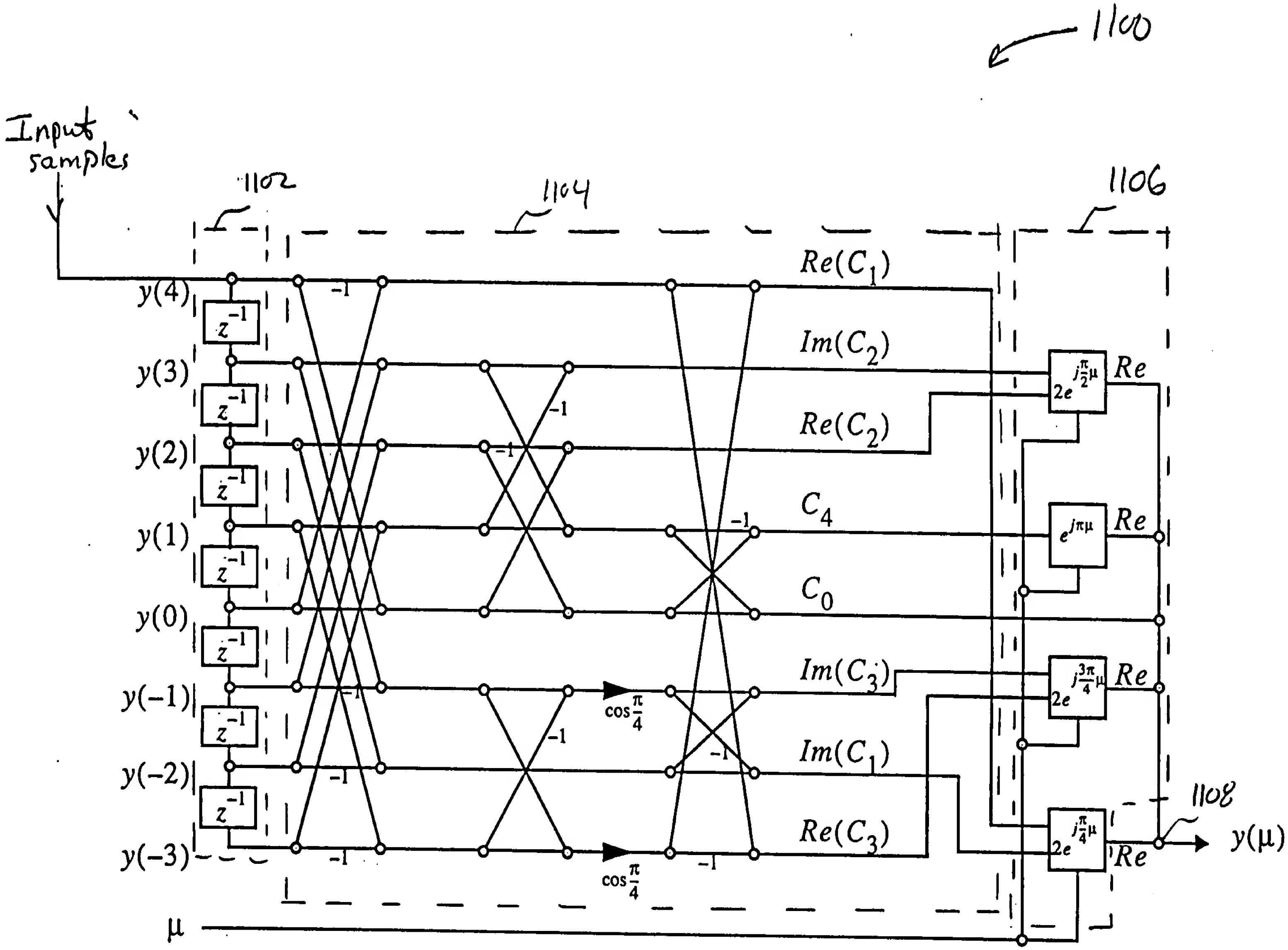

Figure 11 Trigonometric Interpolator with N=8.

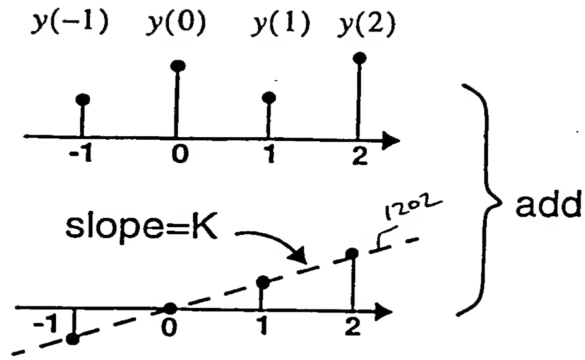

Figure 12 Conceptual modification of input samples.

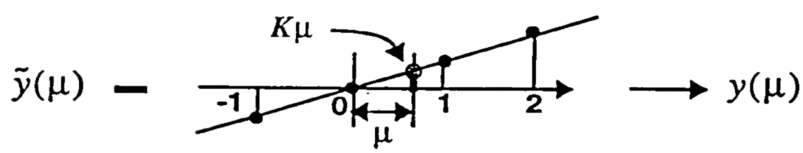

Figure 13 Correcting the offset due to modification of original samples.

1400

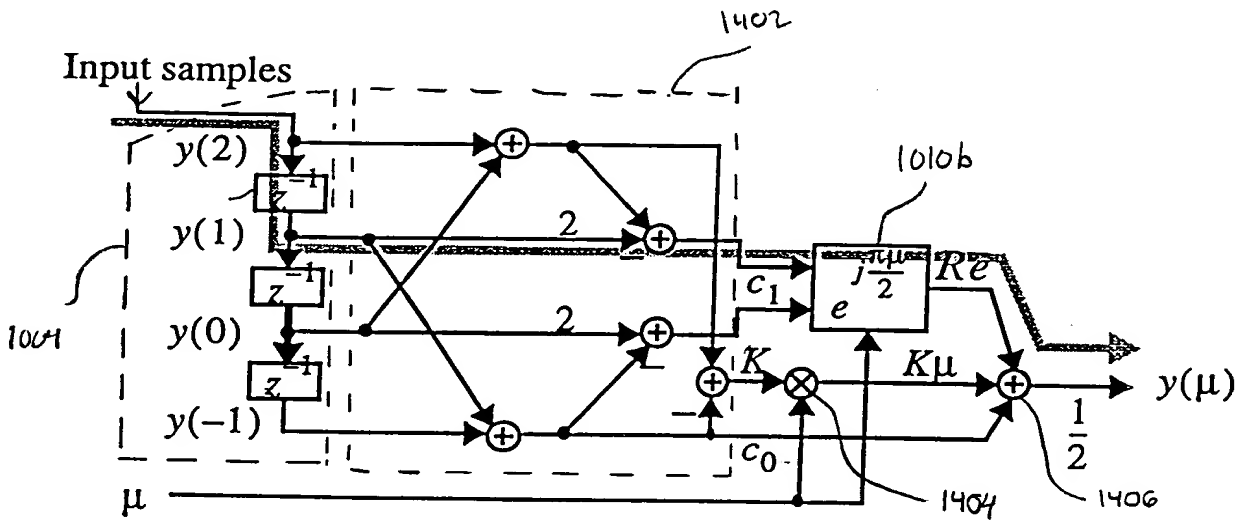

FIG. 14: Trigonometric Interpolator N=4

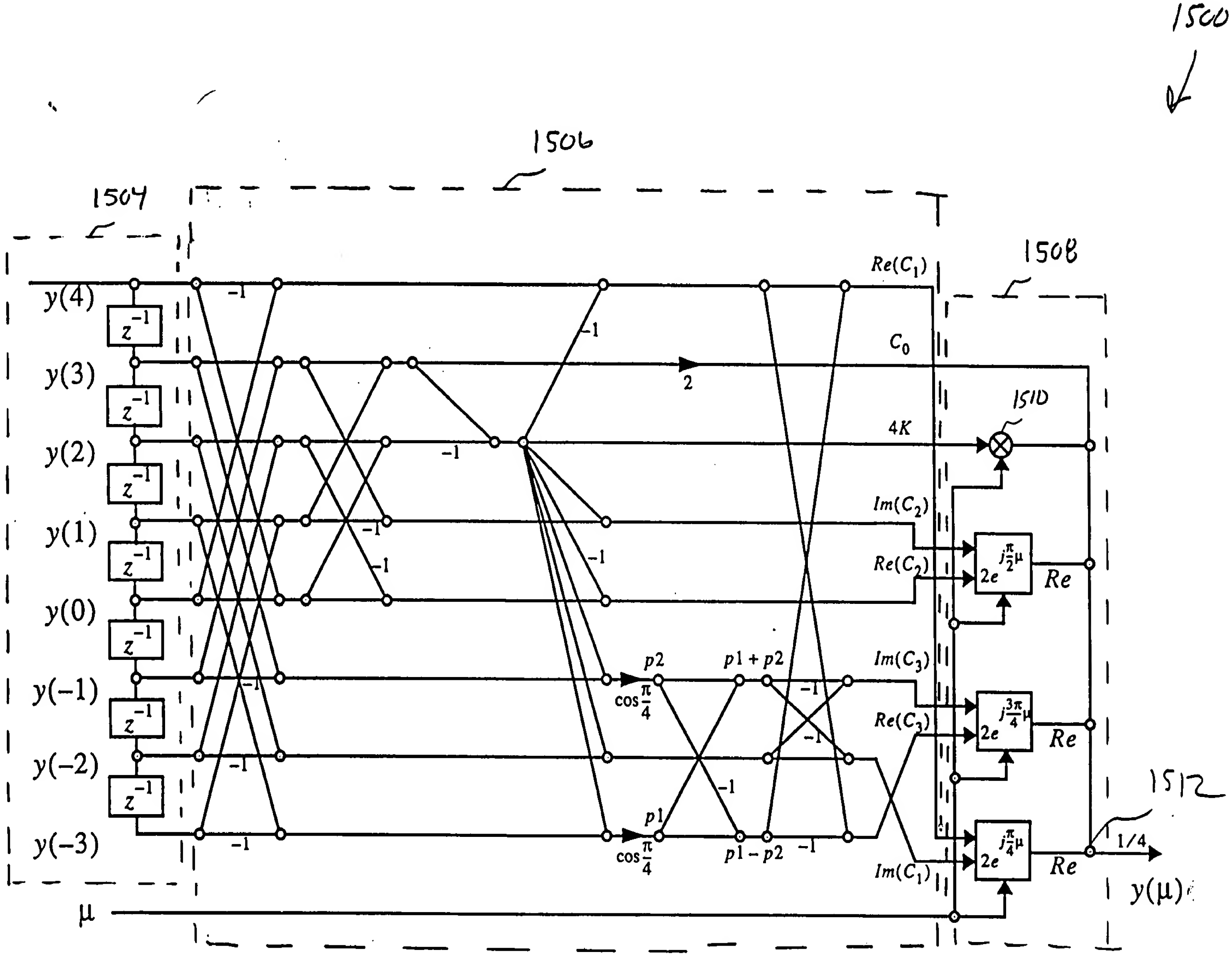

FIG. 15 The modified Trigonometric Interpolator

Interpolation errors are shown in gray.

FIG. 16A: Lagrange cubic

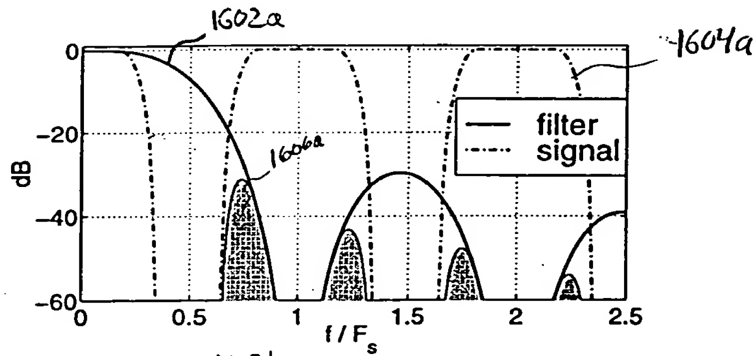

FIG. 16B: Trigonometric Interpolator 1000 (FIG. 10)

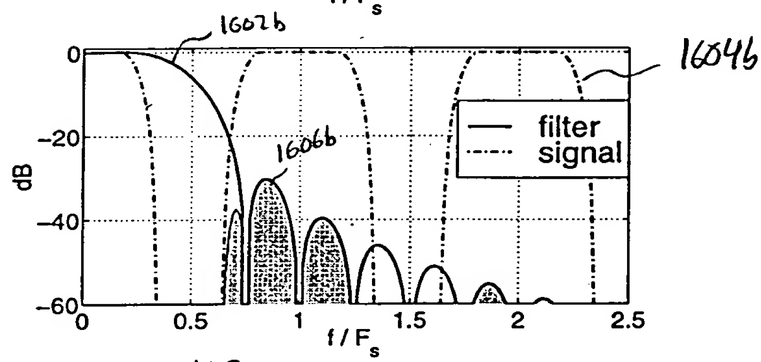

FIG. 16C: Trigonometric Interpolator 1400 (FIG. 14)

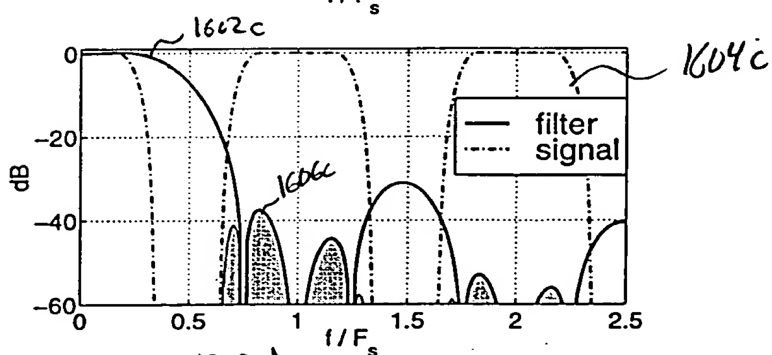

FIG. 16D: Optimal structure

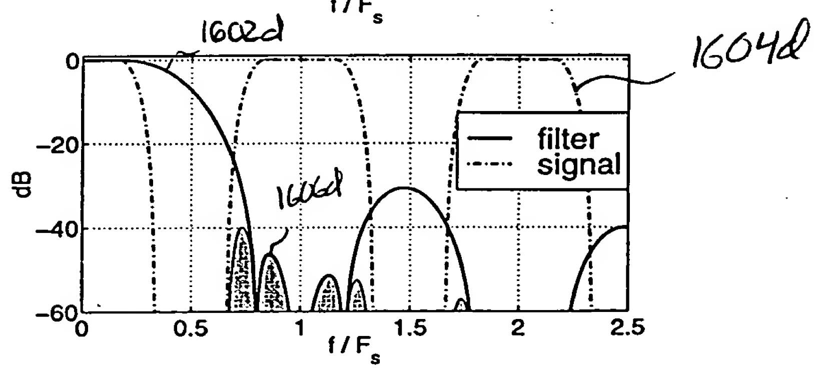

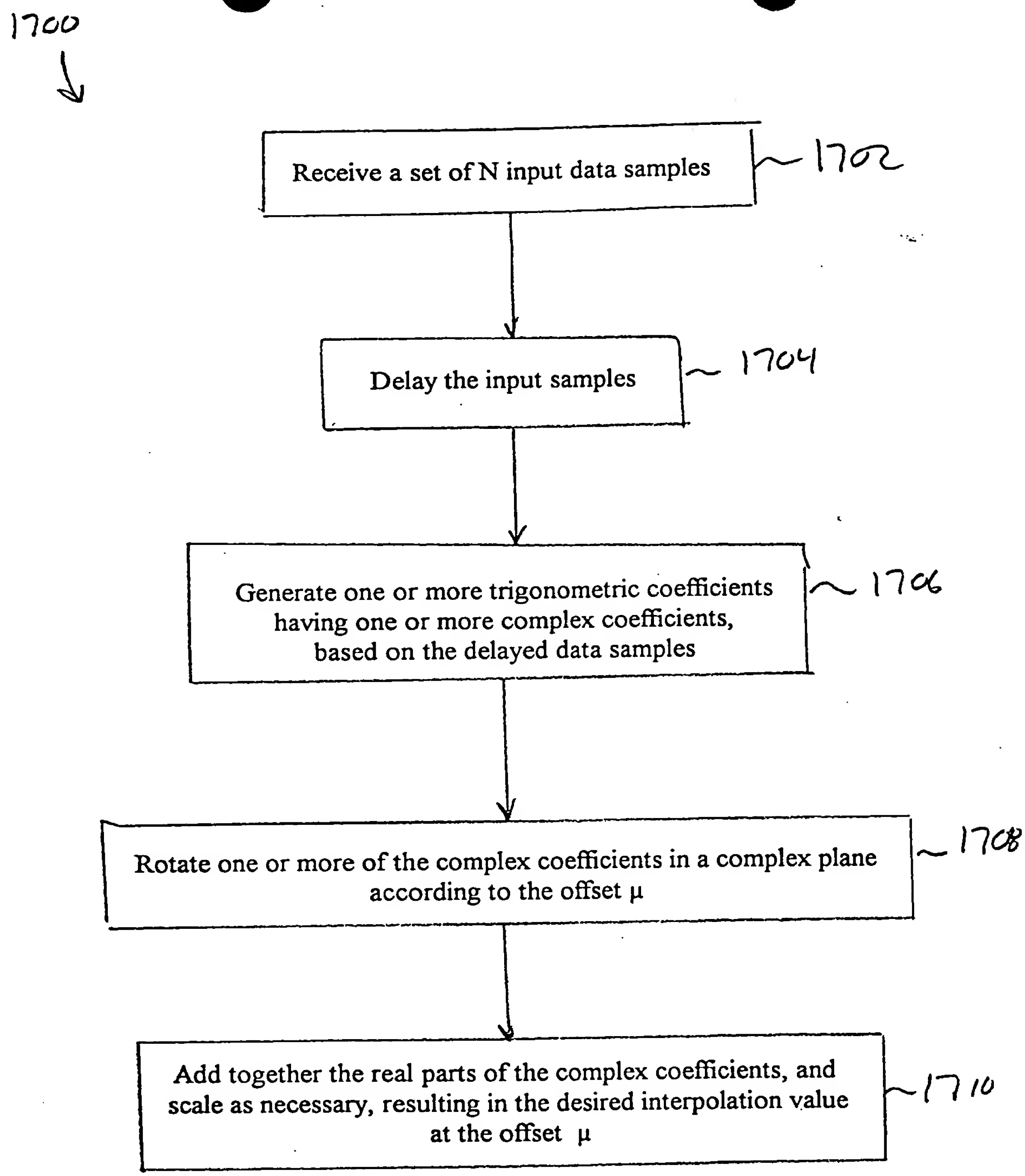
1700
Receive a set of N input data samples
1702
Delay the input samples
1704
Generate one or more trigonometric coefficients having one or more complex coefficients, based on the delayed data samples
1706
Rotate one or more of the complex coefficients in a complex plane according to the offset μ
1708
Add together the real parts of the complex coefficients, and scale as necessary, resulting in the desired interpolation value at the offset μ
1710

FIG. 17

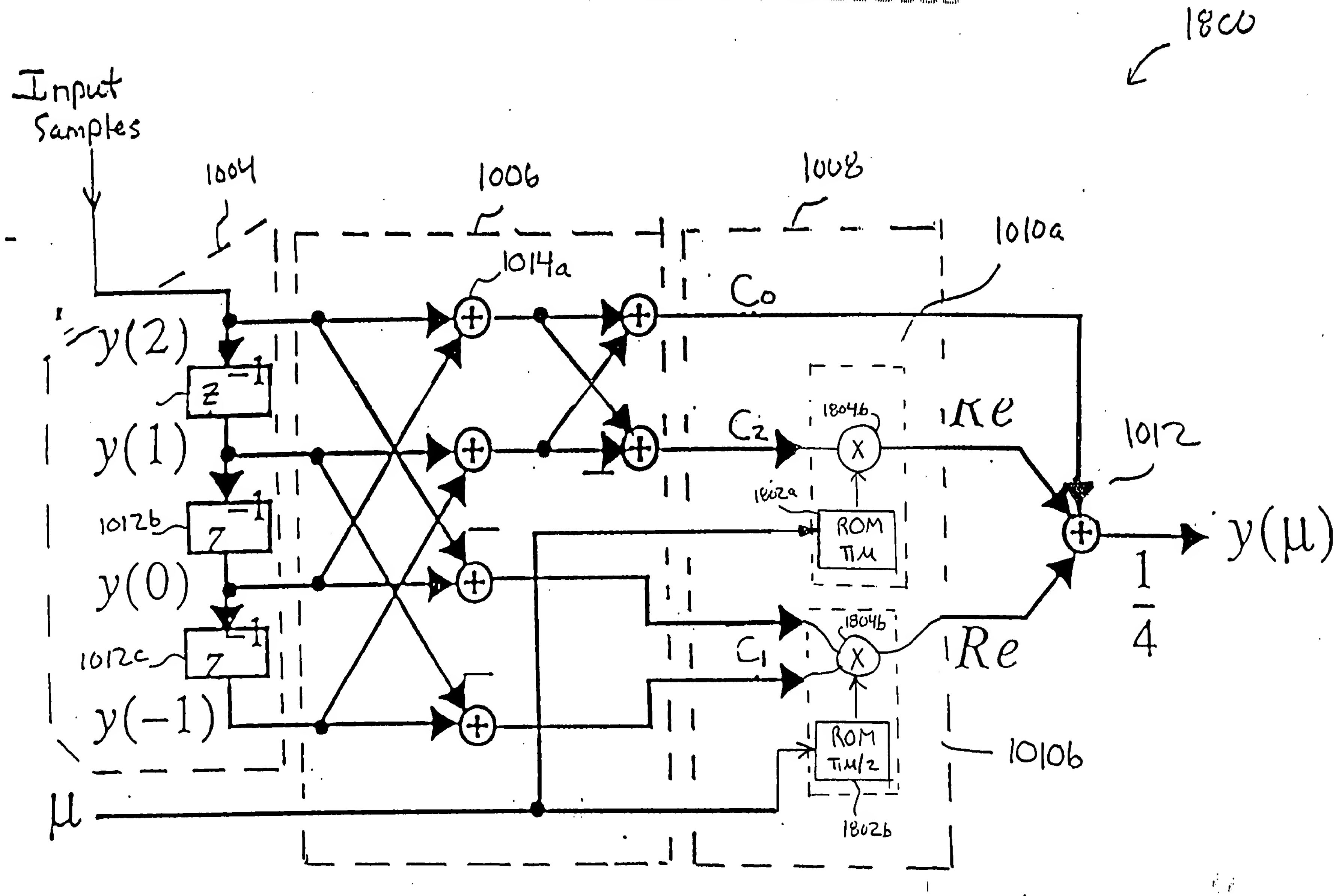
1800
Input Samples
1004
1006
1008
1010a
1014a
C_0
C_2
C_1
y(2)
y(1)
y(0)
y(−1)
z^{-1}
1012b
1012c
1804b
1802a
ROM πμ
ROM πμ/2
1802b
Re
Re
1012
1010b
1/4
y(μ)
μ

FIG. 18

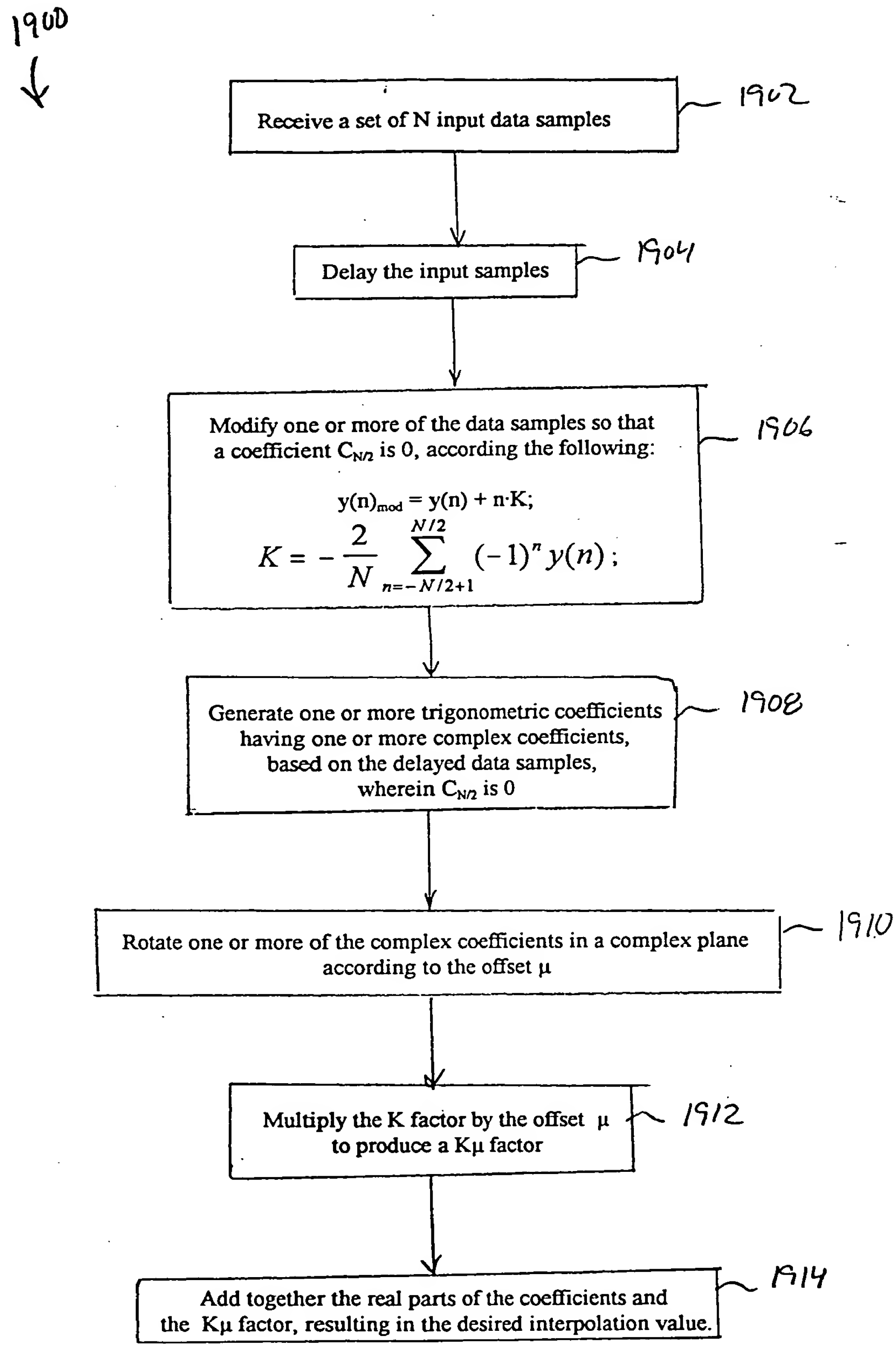
1900
Receive a set of N input data samples
1902
Delay the input samples
1904
Modify one or more of the data samples so that a coefficient $C_{N/2}$ is 0, according the following:
$y(n)_{mod} = y(n) + n \cdot K$;
$K = -\frac{2}{N} \sum_{n=-N/2+1}^{N/2} (-1)^n y(n)$;
1906
Generate one or more trigonometric coefficients having one or more complex coefficients, based on the delayed data samples, wherein $C_{N/2}$ is 0
1908
Rotate one or more of the complex coefficients in a complex plane according to the offset μ
1910
Multiply the K factor by the offset μ to produce a Kμ factor
1912
Add together the real parts of the coefficients and the Kμ factor, resulting in the desired interpolation value.
1914

FIG. 19

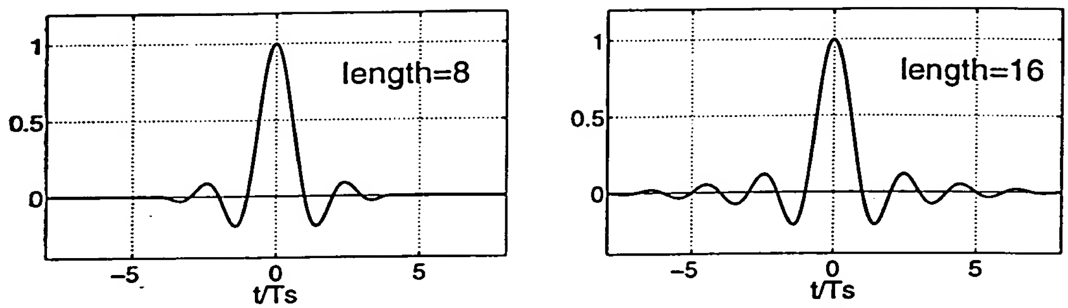

(a) (b)

FIG. 20: Normalized Impulse responses *f* of the interpolation filters.

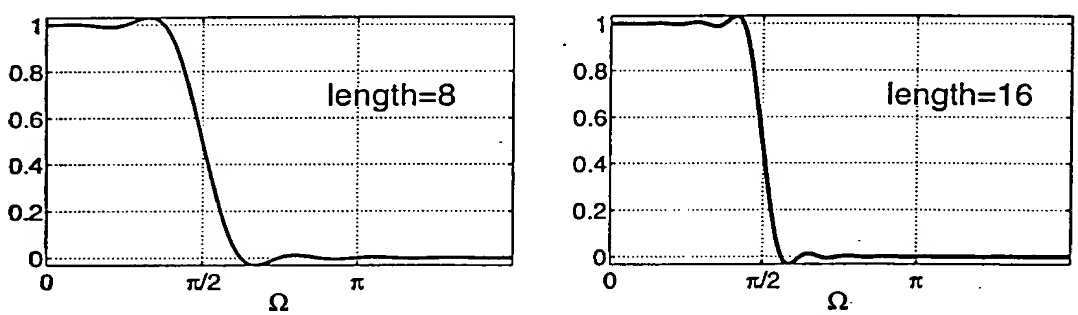

(a) (b)

FIG. 21: Normalized Frequency responses *F* of the interpolation filters.

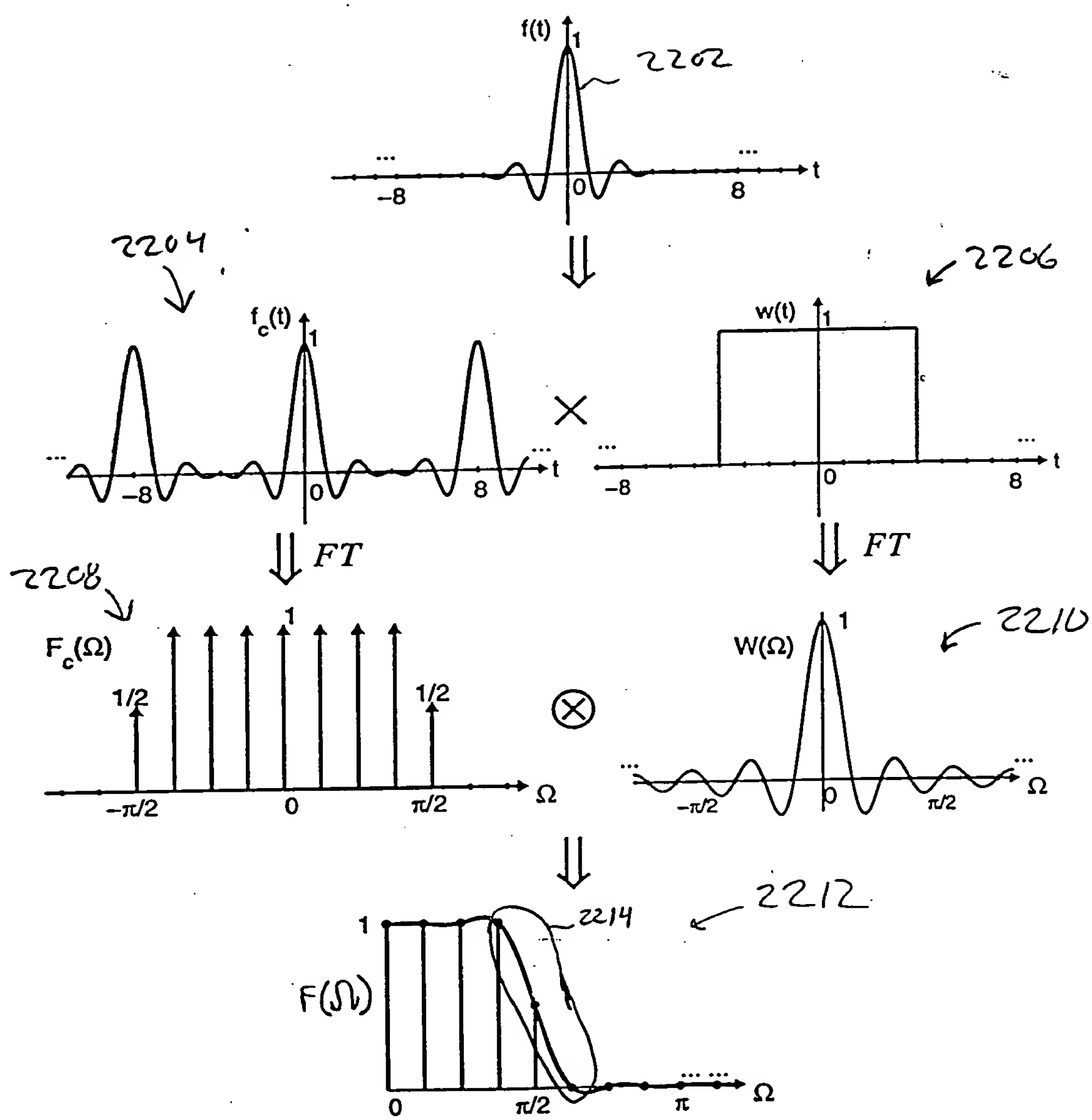

FIG. 22: Analysis of the frequency responses.

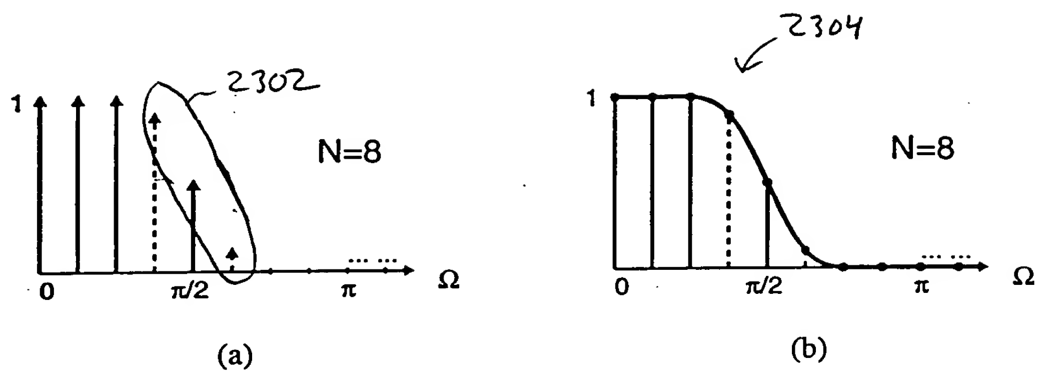

FIG.23 Effect of a more gradual transition at the band edge.

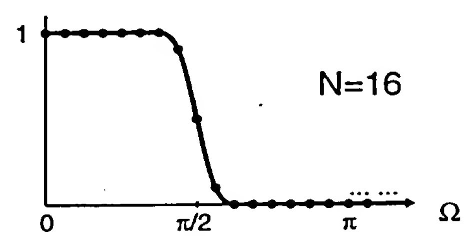

FIG.24 Reducing the transition bandwidth by increasing N.

3-4b, in which $N = 8$.

FIG. 25A

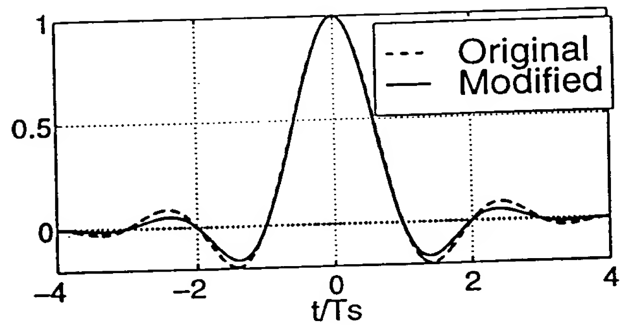

FIG. 25B

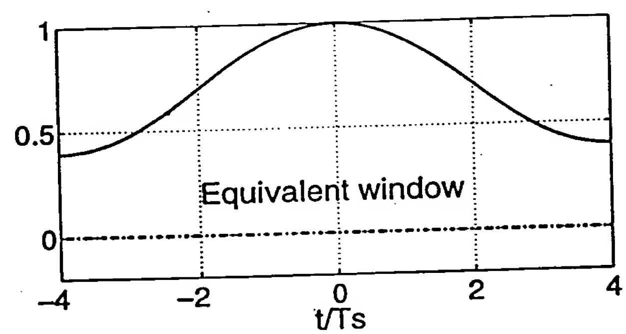

FIG. 25A-B: (A) Impulse response of the original filter and the modified filter: (B) The equivalent window.

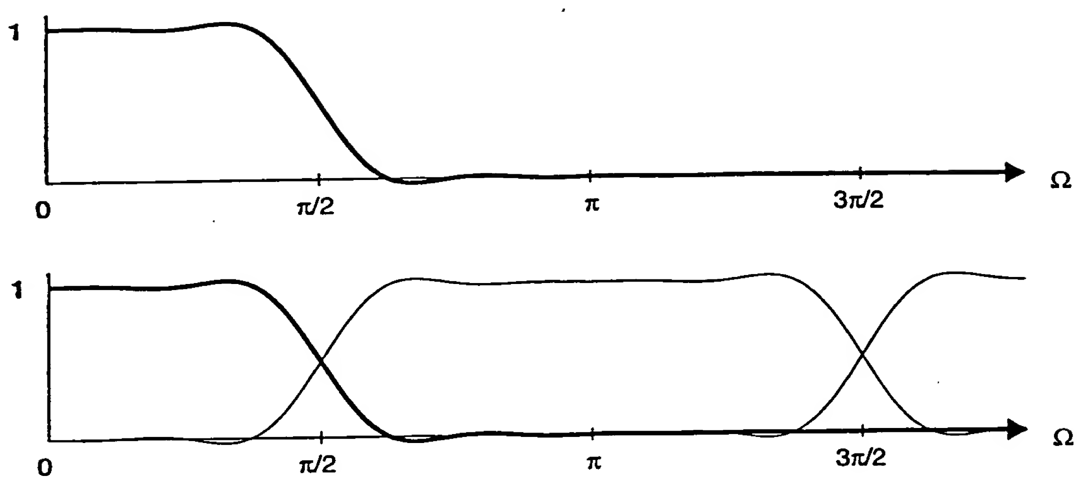

FIG. 26 Forming the frequency response of the discrete-time fractional-delay filter.

FIG. 27A

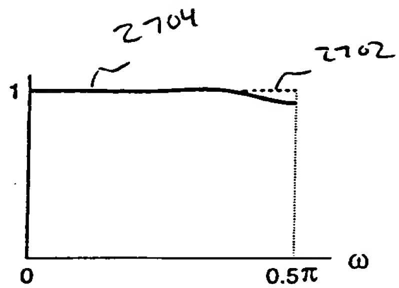

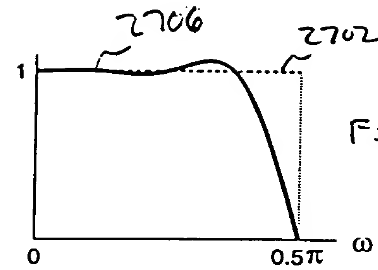

FIG. 27B

FIG. 27A-B: Fractional-delay filter with (A) μ=0.12 and (B) μ=0.5, using the preliminary N=8 interpolator.

FIG. 28A

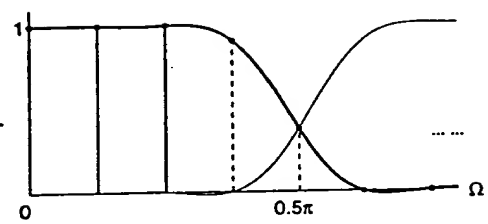

μ=0.12

FIG 28B

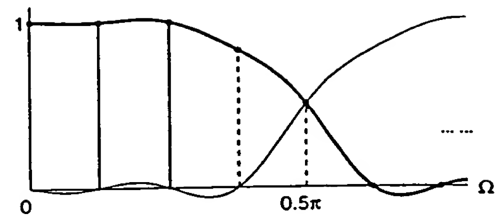

μ=0.5

FIG. 28C

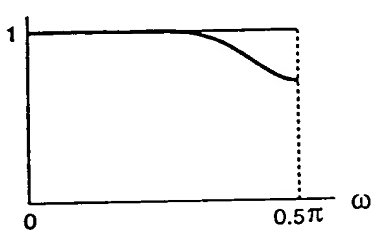

μ=0.12

FIG. 28D

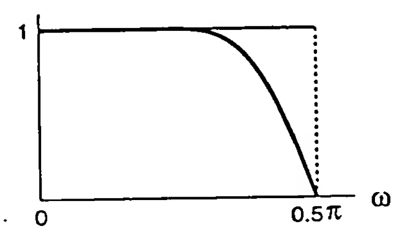

μ=0.5

FIG. 29A

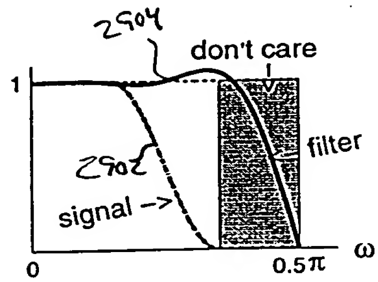

FIG. 29B

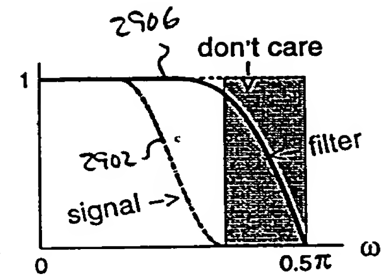

FIG. 29A-B: $F_{\mu}(\omega)$, with μ=0.5, N=8, (A) before and (B) after optimization.

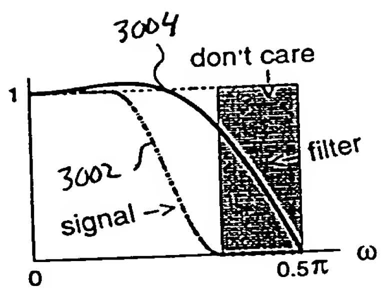

FIG. 30A

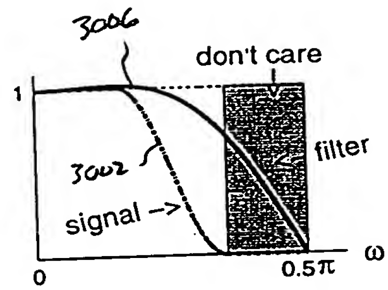

FIG. 30B

FIG. 30A-B $F_{\mu}(\omega)$ for μ=0.5, N=4, (A) before and (B) after modification.

FIG.31A

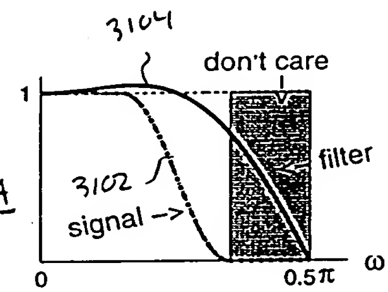

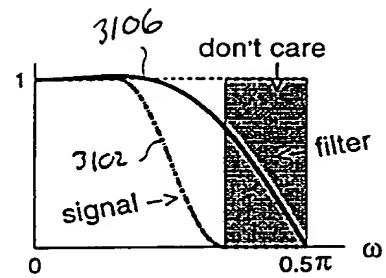

FIG.31B

FIG.31A-B $F_\mu(\omega)$, μ=0.5, simplified N=4 structure, A before and B after modification.

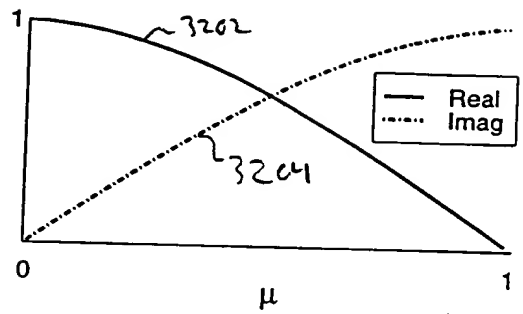

FIG. 32: Real and imaginary components of the $\hat{F}_{\mu}(1)e^{j\frac{\pi}{2}\mu}$ value.

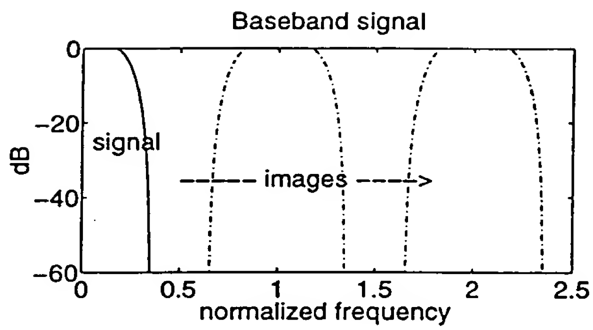

FIG. 33: Signal with two samples/symbol and 40% excess bandwidth.

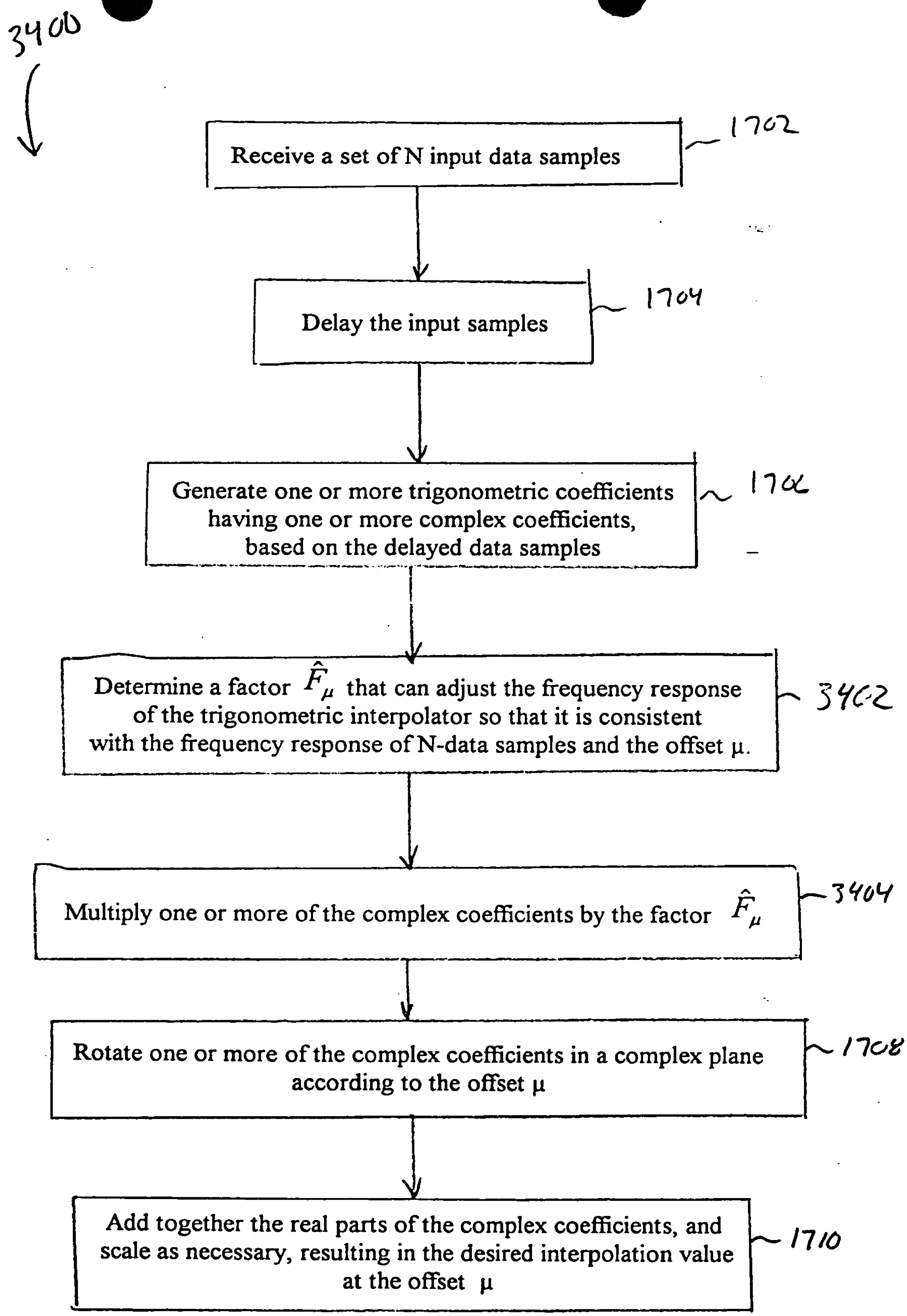
3400
Receive a set of N input data samples
1702
Delay the input samples
1704
Generate one or more trigonometric coefficients having one or more complex coefficients, based on the delayed data samples
1706
Determine a factor $\hat{F}_{\mu}$ that can adjust the frequency response of the trigonometric interpolator so that it is consistent with the frequency response of N-data samples and the offset μ.
3402
Multiply one or more of the complex coefficients by the factor $\hat{F}_{\mu}$
3404
Rotate one or more of the complex coefficients in a complex plane according to the offset μ
1708
Add together the real parts of the complex coefficients, and scale as necessary, resulting in the desired interpolation value at the offset μ
1710

FIG. 34

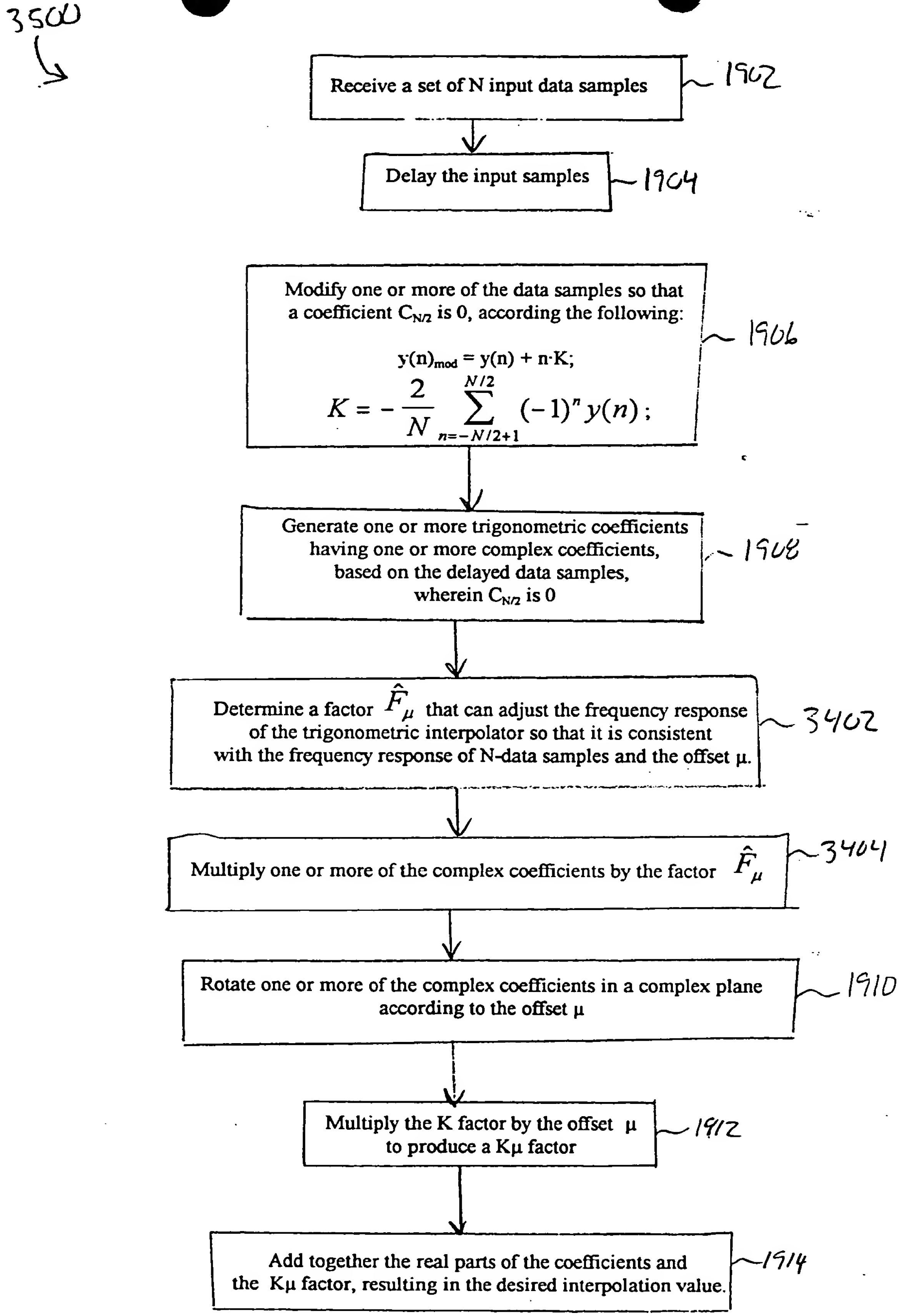
3500
Receive a set of N input data samples
1902
Delay the input samples
1904
Modify one or more of the data samples so that a coefficient $C_{N/2}$ is 0, according the following:
$y(n)_{mod} = y(n) + n \cdot K;$
$K = -\frac{2}{N} \sum_{n=-N/2+1}^{N/2} (-1)^n y(n);$
1906
Generate one or more trigonometric coefficients having one or more complex coefficients, based on the delayed data samples, wherein $C_{N/2}$ is 0
1908
Determine a factor $\hat{F}_\mu$ that can adjust the frequency response of the trigonometric interpolator so that it is consistent with the frequency response of N-data samples and the offset μ.
3402
Multiply one or more of the complex coefficients by the factor $\hat{F}_\mu$
3404
Rotate one or more of the complex coefficients in a complex plane according to the offset μ
1910
Multiply the K factor by the offset μ to produce a Kμ factor
1912
Add together the real parts of the coefficients and the Kμ factor, resulting in the desired interpolation value.
1914

FIG. 35

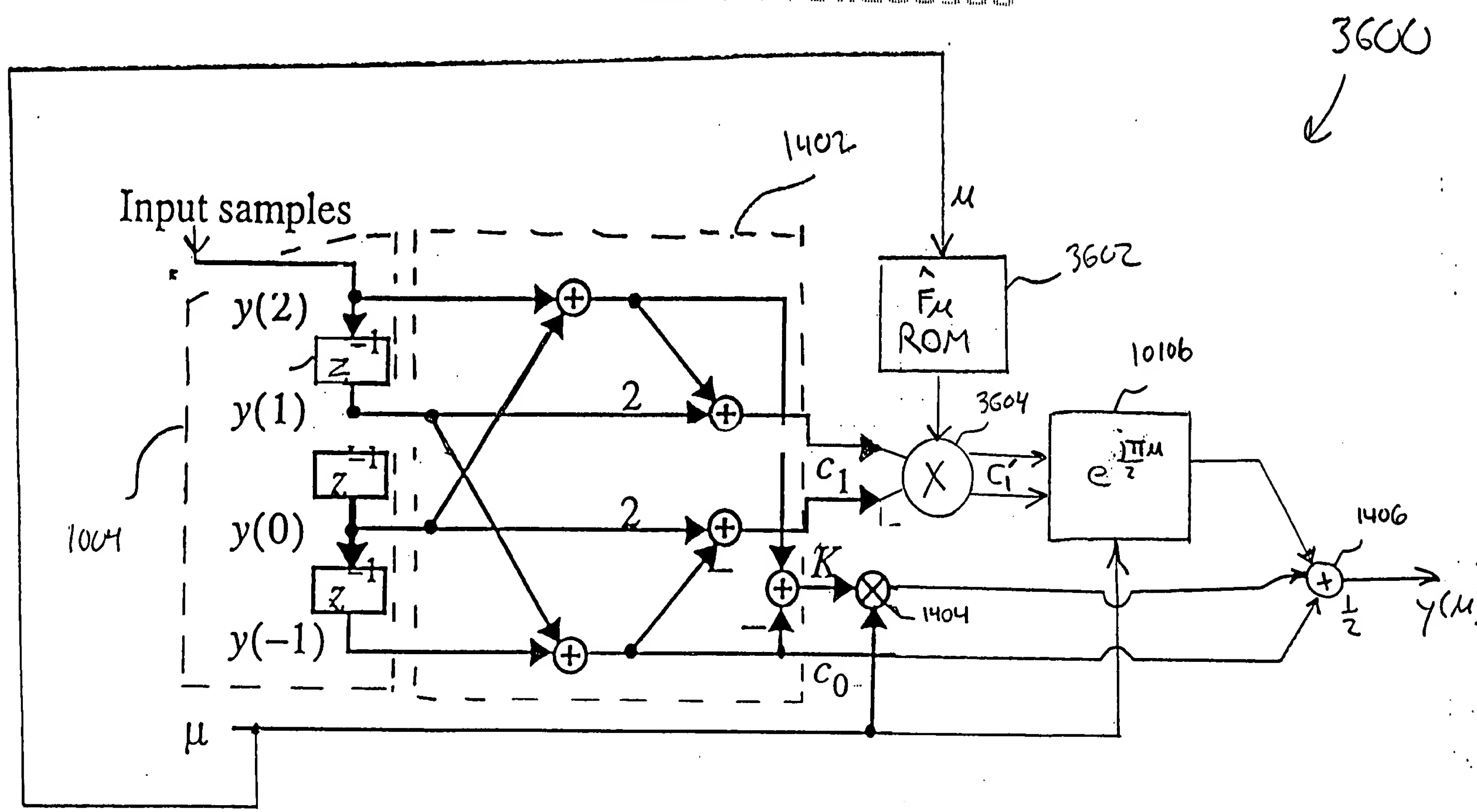

FIG. 36 The optimized structure for N=4.

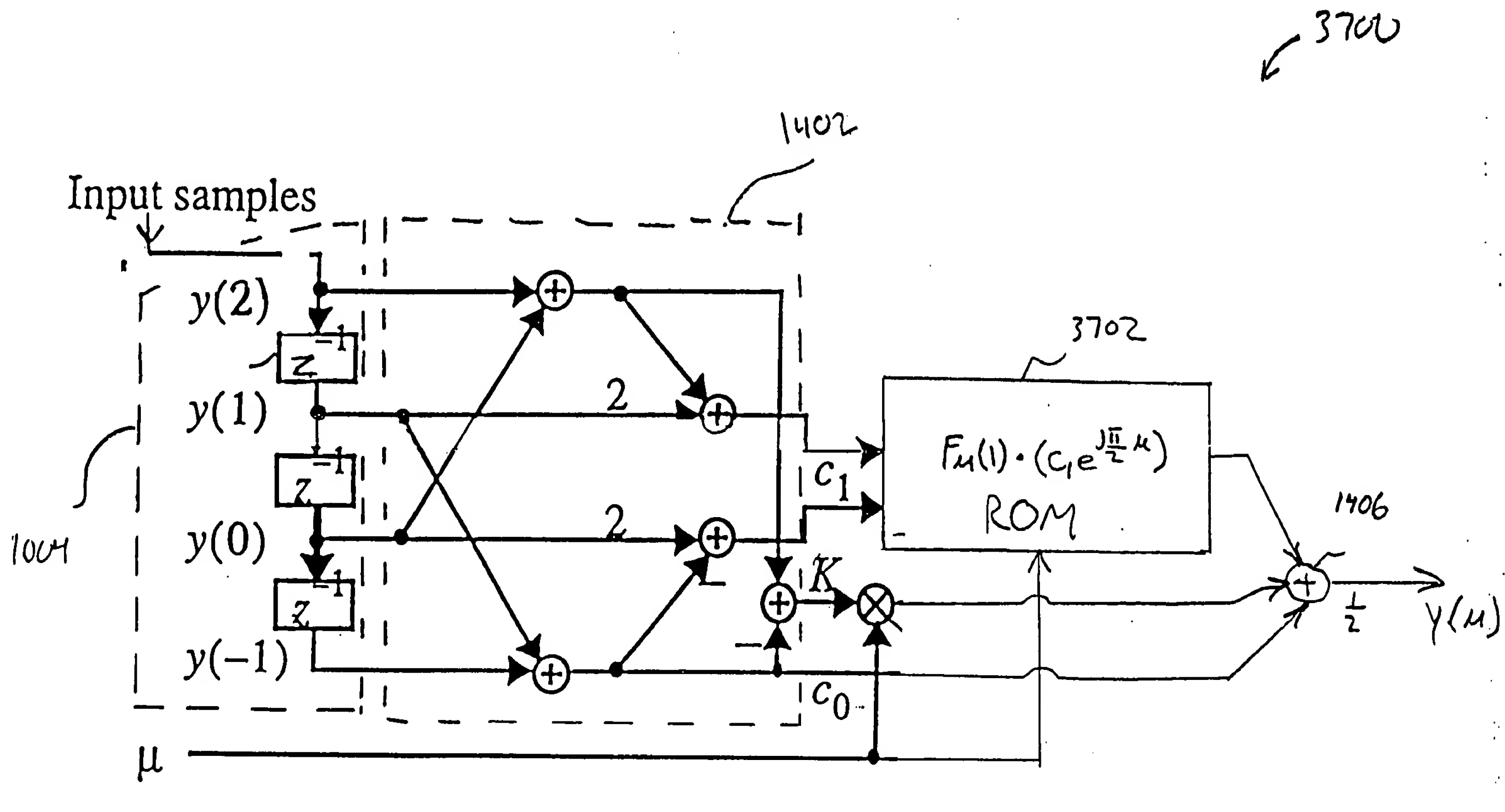

FIG. 37: The optimized structure for $N=4$.

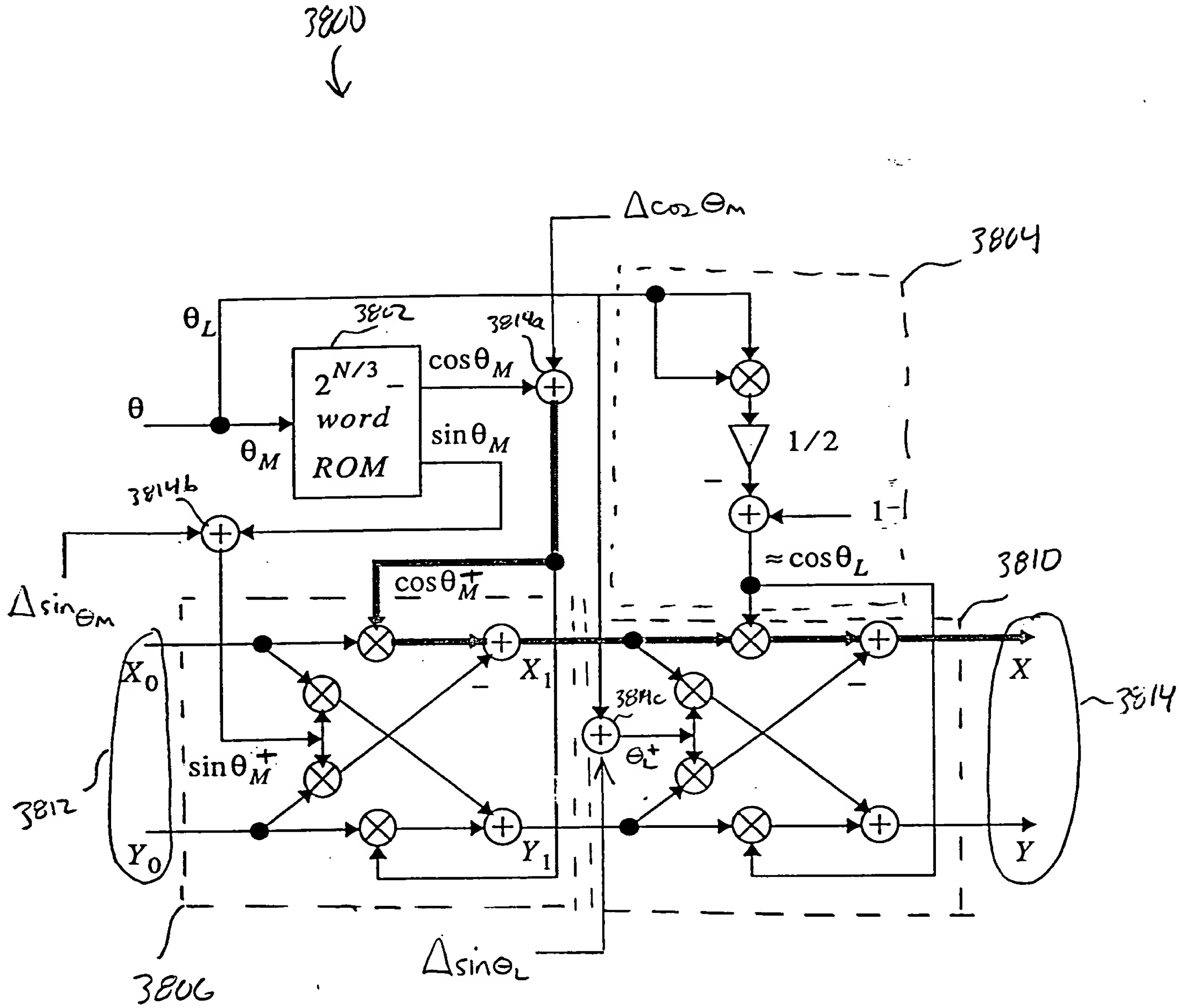
3800
Δcos θM
3804
θL
3802
3814a
2^N/3 - word ROM
cosθM
θ
θM
sinθM
1/2
3814b
1-
≈cosθL
Δsin θM
cosθM+
3810
X0
X1
X
3814
3814c
θL+
sinθM+
3812
Y0
Y1
Y
3806
Δsin θL

FIG. 38

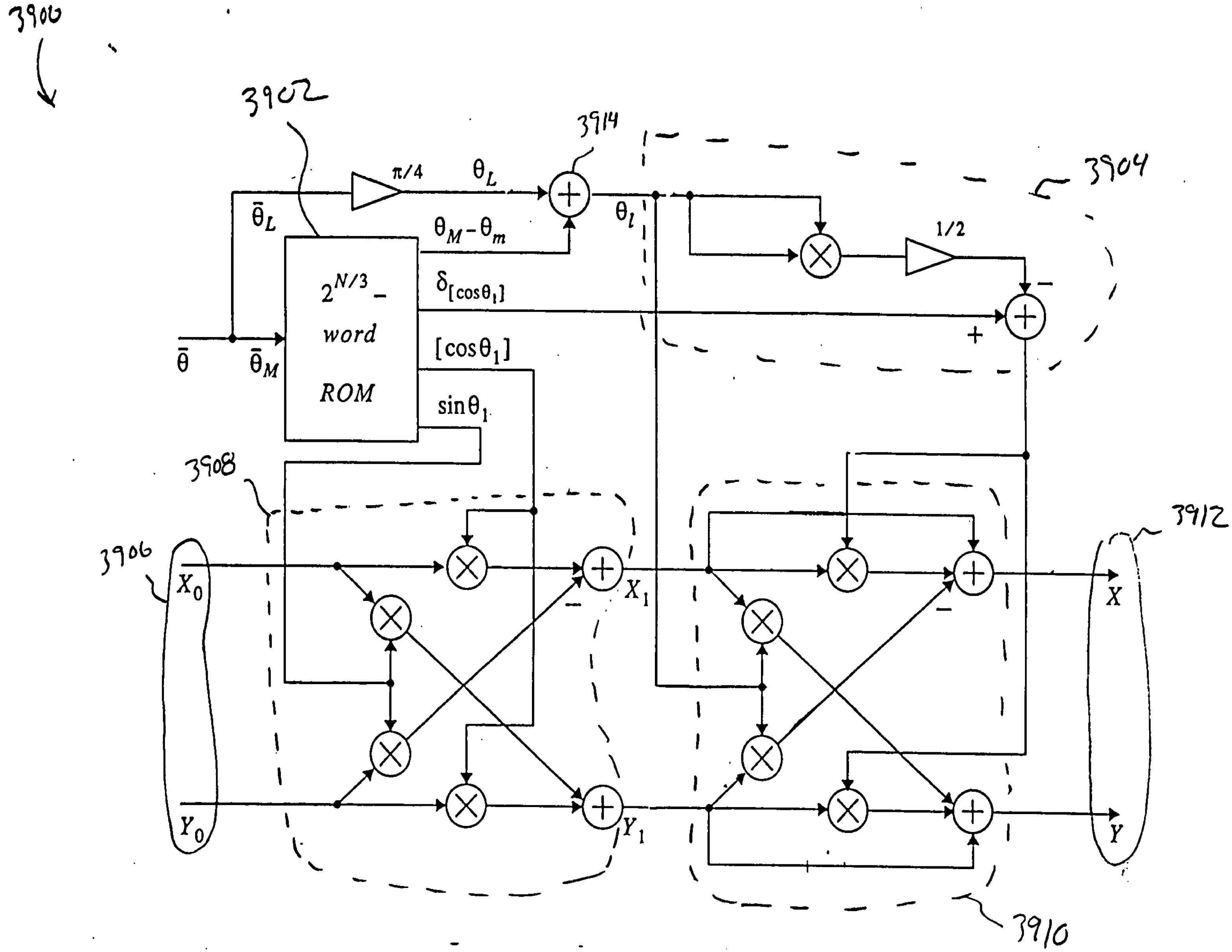
3900
3902
3914
3904
π/4
1/2
θ̄
θ̄_L
θ̄_M
θ_L
θ_M-θ_m
θ_l
δ[cosθ_1]
[cosθ_1]
sinθ_1
2^{N/3}-
word
ROM
+
-
3908
3906
3910
3912
X_0
Y_0
X_1
Y_1
X
Y

FIG. 39

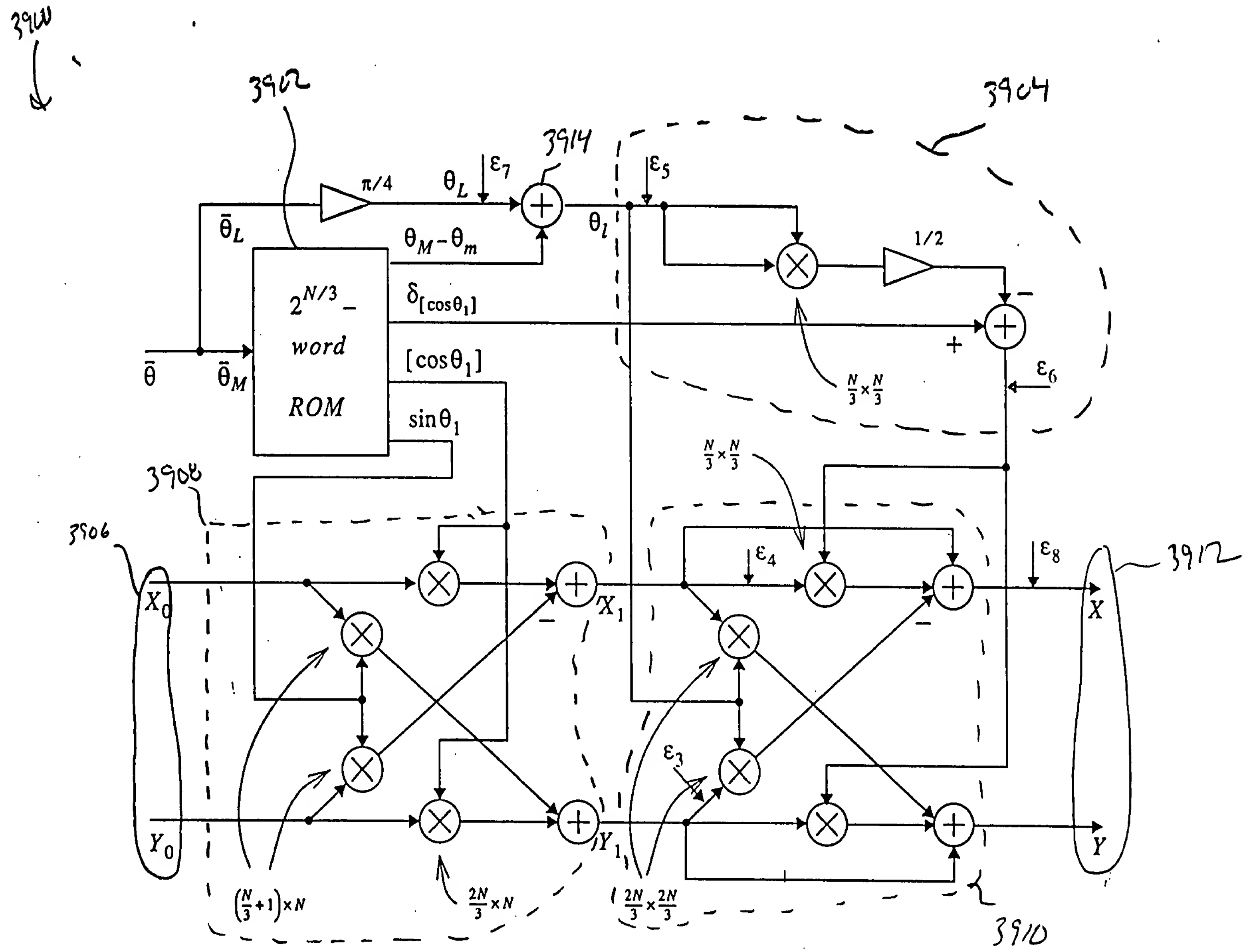
3900
3902
3904
3914
3906
3908
3910
3912
$2^{N/3}$-word ROM
$\bar{\theta}$
$\bar{\theta}_L$
$\bar{\theta}_M$
$\pi/4$
θ_L
ε_7
$\theta_M-\theta_m$
$\delta_{[\cos\theta_1]}$
$[\cos\theta_1]$
$\sin\theta_1$
θ_l
ε_5
1/2
ε_6
$\frac{N}{3}\times\frac{N}{3}$
ε_4
ε_3
ε_8
X_0
Y_0
X_1
Y_1
X
Y
$(\frac{N}{3}+1)\times N$
$\frac{2N}{3}\times N$
$\frac{2N}{3}\times\frac{2N}{3}$

FIG. 40

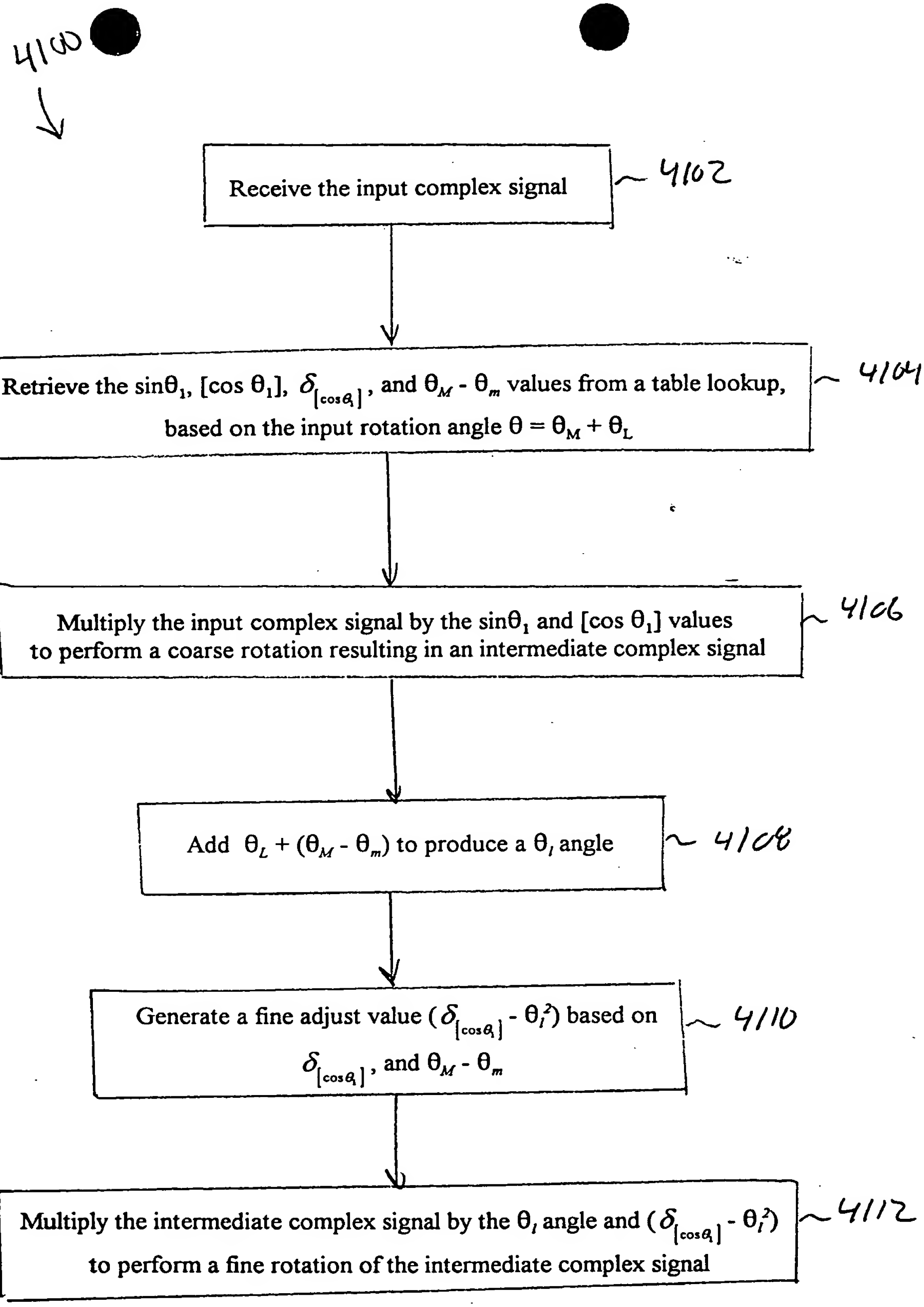

4100
Receive the input complex signal
4102
Retrieve the $\sin\theta_1$, $[\cos\theta_1]$, $\delta_{[\cos\theta_1]}$, and $\theta_M - \theta_m$ values from a table lookup, based on the input rotation angle $\theta = \theta_M + \theta_L$
4104
Multiply the input complex signal by the $\sin\theta_1$ and $[\cos\theta_1]$ values to perform a coarse rotation resulting in an intermediate complex signal
4106
Add $\theta_L + (\theta_M - \theta_m)$ to produce a θ_l angle
4108
Generate a fine adjust value $(\delta_{[\cos\theta_1]} - \theta_l^2)$ based on $\delta_{[\cos\theta_1]}$, and $\theta_M - \theta_m$
4110
Multiply the intermediate complex signal by the θ_l angle and $(\delta_{[\cos\theta_1]} - \theta_l^2)$ to perform a fine rotation of the intermediate complex signal
4112

FIG. 41

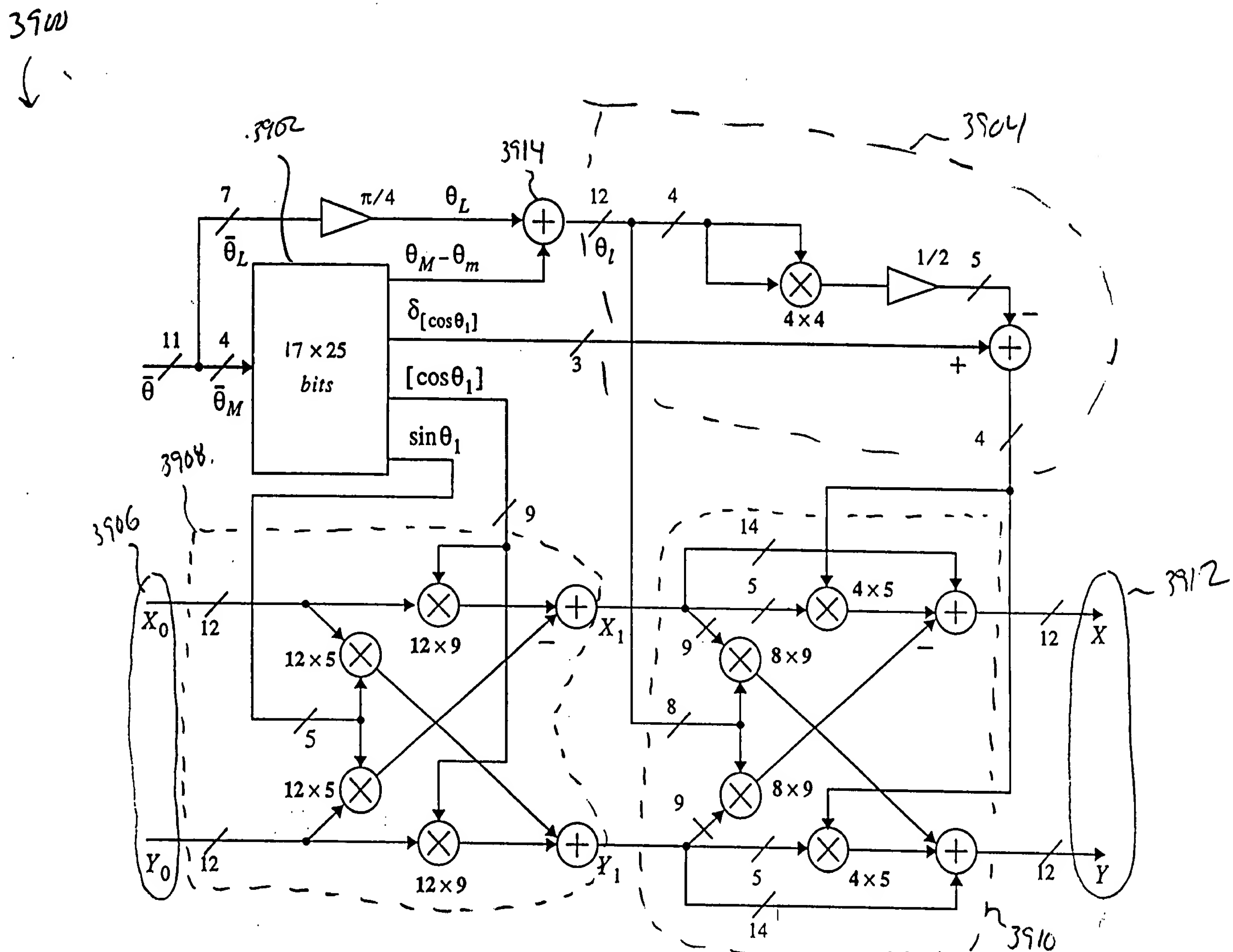

FIG. 42 The internal wordlength of the structure that achieved 90.36 dB SFDR.

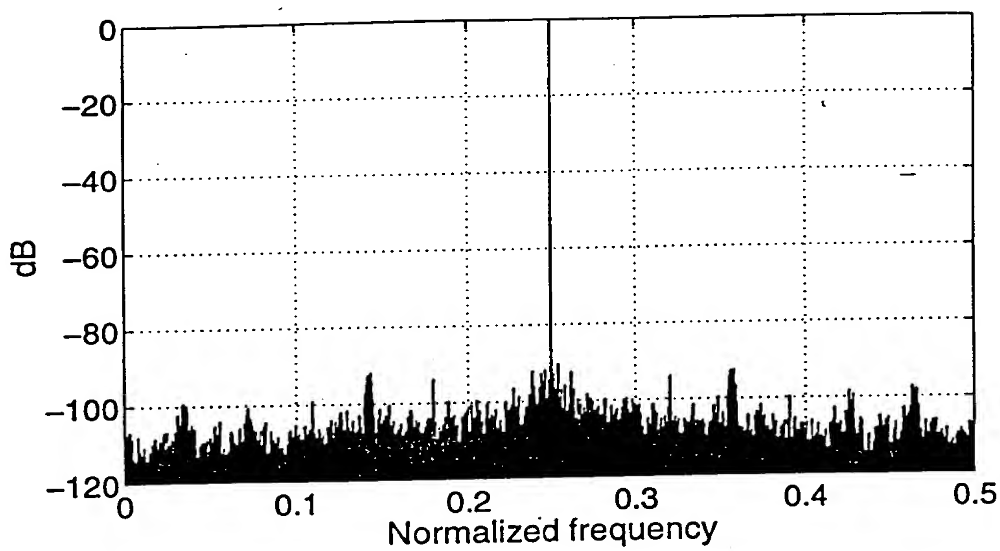

FIG. 43 Output spectrum showing 90.36 dB SFDR.

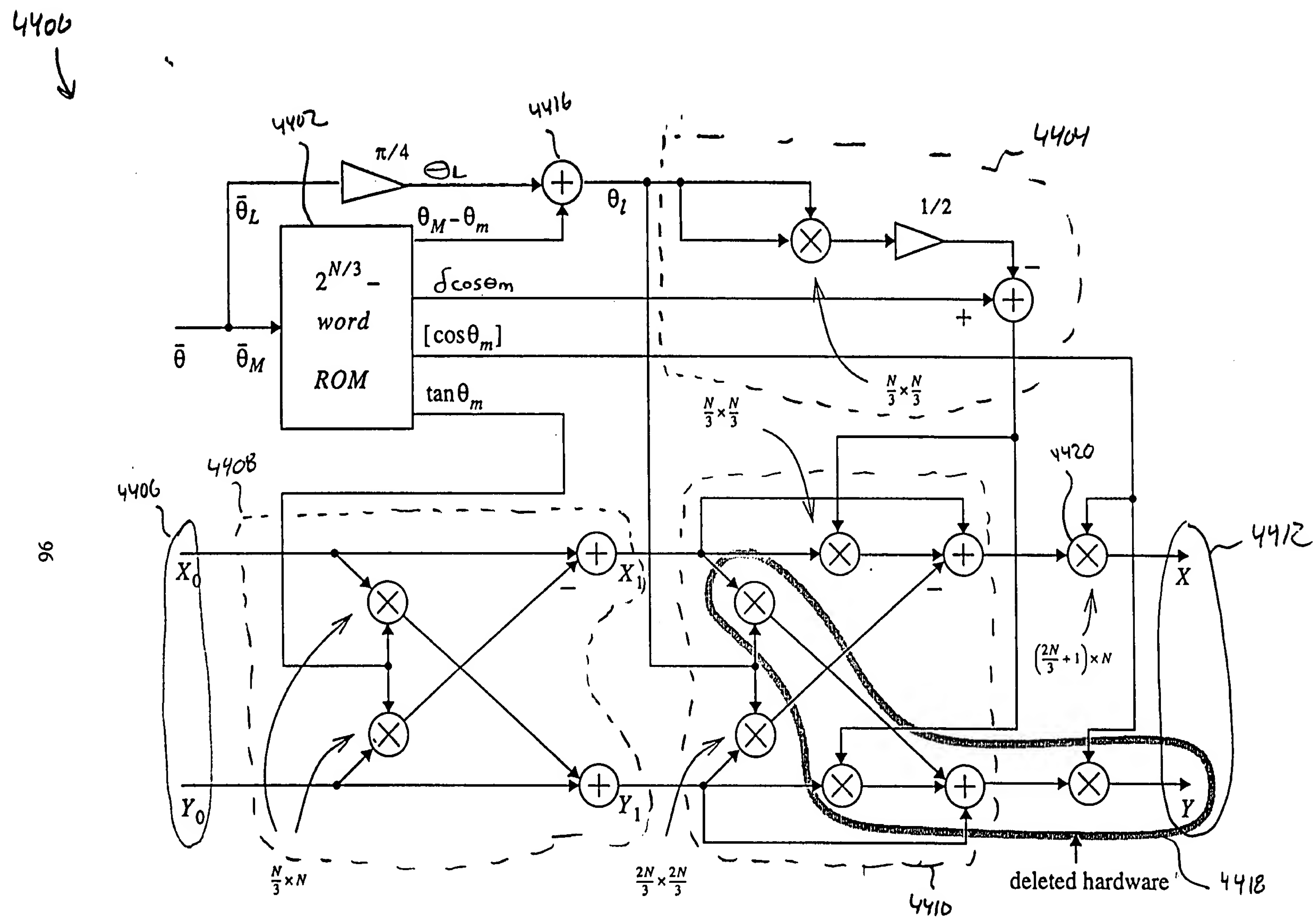

FIG. 44 A modified architecture when only one output is needed.

4500

Receive the input complex signal 4502

Retrieve the $\tan\theta_m$ [$\cos\theta_m$], $\delta_{\cos\theta_m}$, and $(\theta_M - \theta_m)$ values from a table lookup, based on the input rotation angle θ 4504

Multiply the input complex signal by the $\tan\theta_m$ value to perform a coarse rotation resulting in an intermediate complex signal 4506

Add $\theta_L + (\theta_M - \theta_m)$ to produce a θ_l angle 4508

Generate a fine adjust value ($\delta_{\cos\theta_m} - \theta_l^2$) based on $\delta_{\cos\theta_m}$, and $\theta_M - \theta_m$ 4510

Multiply the intermediate complex signal by the θ_l angle and ($\delta_{\cos\theta_m} - \theta_l^2$) to perform a fine rotation of the intermediate complex signal 4512

Scale the desired (X or Y) value of the output signal by [$\cos\theta_m$] 4514

FIG. 45

460

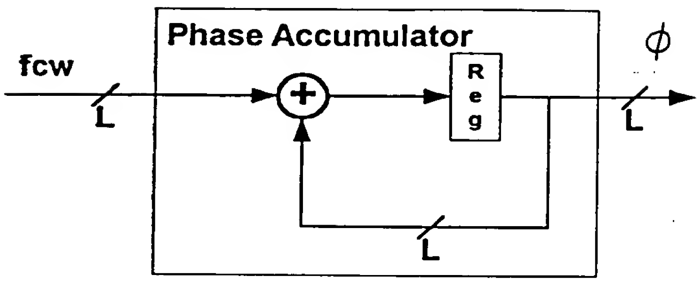

where the adder is an overflowing accumulator.

FIG. 46

4700

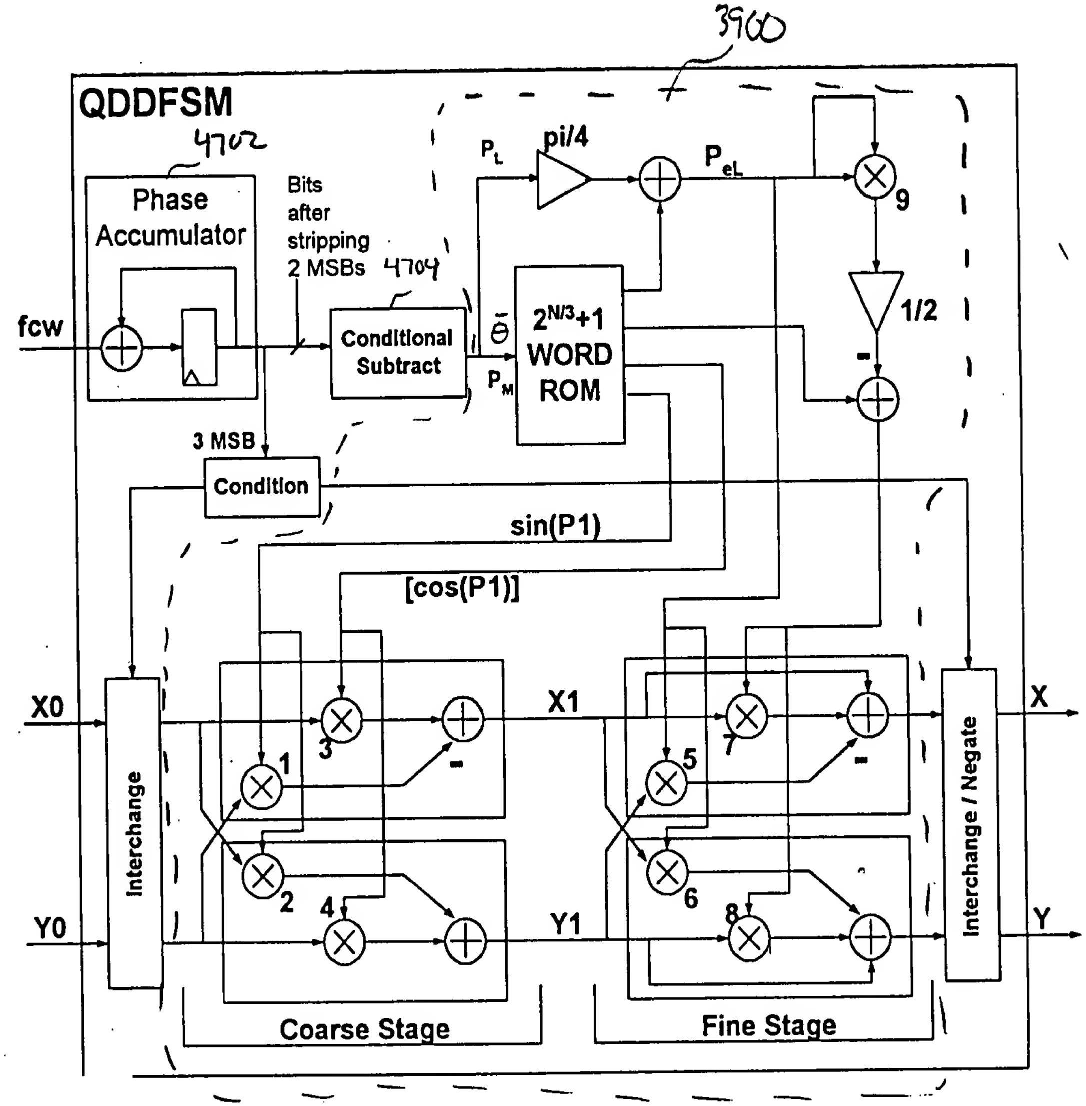
3900
QDDFSM
4702
Phase Accumulator
fcw
Bits after stripping 2 MSBs
4704
Conditional Subtract
3 MSB
Condition
P_L
pi/4
P_{eL}
9
1/2
$\bar{\theta}$
P_M
$2^{N/3}+1$ WORD ROM
sin(P1)
[cos(P1)]
X0
Y0
Interchange
1
2
3
4
X1
Y1
5
6
7
8
Coarse Stage
Fine Stage
Interchange / Negate
X
Y

FIG 47

4800

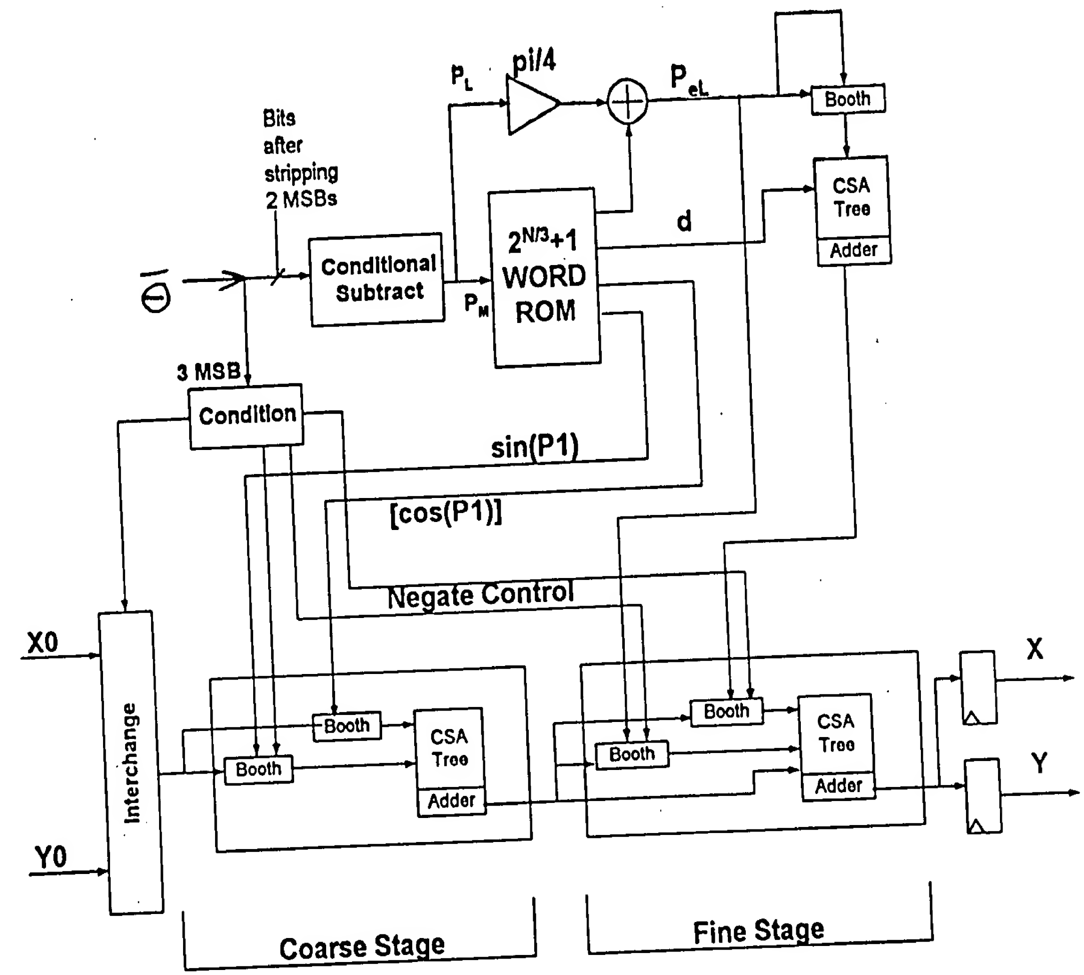
Bits
after
stripping
2 MSBs
$\overline{\Theta}$
Conditional Subtract
P_L
pi/4
P_{eL}
P_M
$2^{N/3}+1$ WORD ROM
d
Booth
CSA Tree
Adder
3 MSB
Condition
sin(P1)
[cos(P1)]
Negate Control
X0
Y0
Interchange
Booth
CSA Tree
Adder
X
Y
Coarse Stage
Fine Stage

FIG. 48

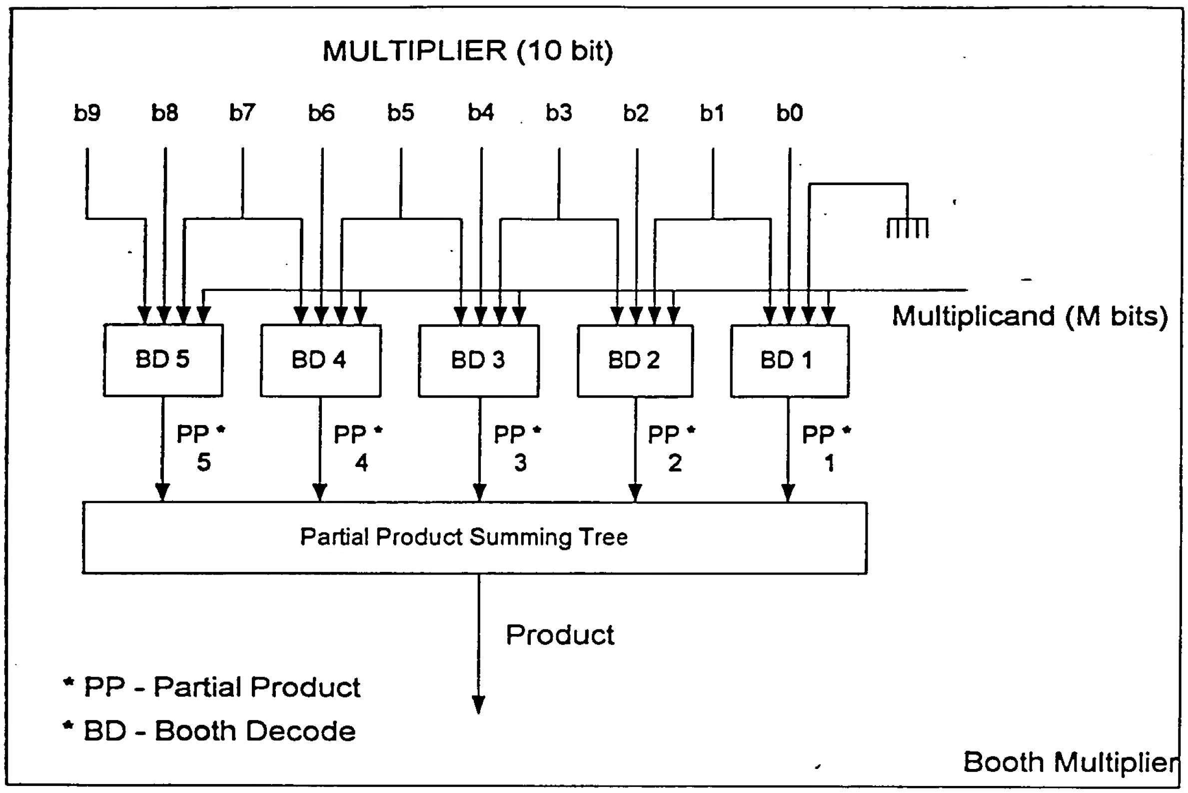
MULTIPLIER (10 bit)
b9
b8
b7
b6
b5
b4
b3
b2
b1
b0
Multiplicand (M bits)
BD 5
BD 4
BD 3
BD 2
BD 1
PP * 5
PP * 4
PP * 3
PP * 2
PP * 1
Partial Product Summing Tree
Product
* PP - Partial Product
* BD - Booth Decode
Booth Multiplier

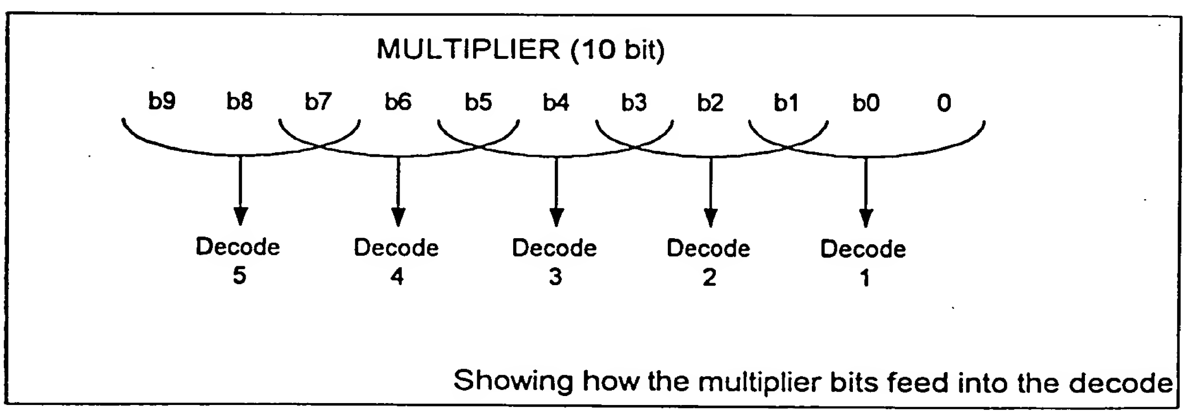
MULTIPLIER (10 bit)
b9
b8
b7
b6
b5
b4
b3
b2
b1
b0
0
Decode 5
Decode 4
Decode 3
Decode 2
Decode 1
Showing how the multiplier bits feed into the decode

FIG. 49

5000

Original Booth Table

5002

b2	b1	b0	PP
0	0	0	0*A
0	0	1	1*A
0	1	0	1*A
0	1	1	2*A
1	0	0	-2*A
1	0	1	-1*A
1	1	0	-1*A
1	1	1	0*A

FIG. 50

5100

Negating Booth Table

5102

b2	b1	b0	PP
0	0	0	0*A
0	0	1	-1*A
0	1	0	-1*A
0	1	1	-2*A
1	0	0	2*A
1	0	1	1*A
1	1	0	1*A
1	1	1	0*A

FIG. 51

5200

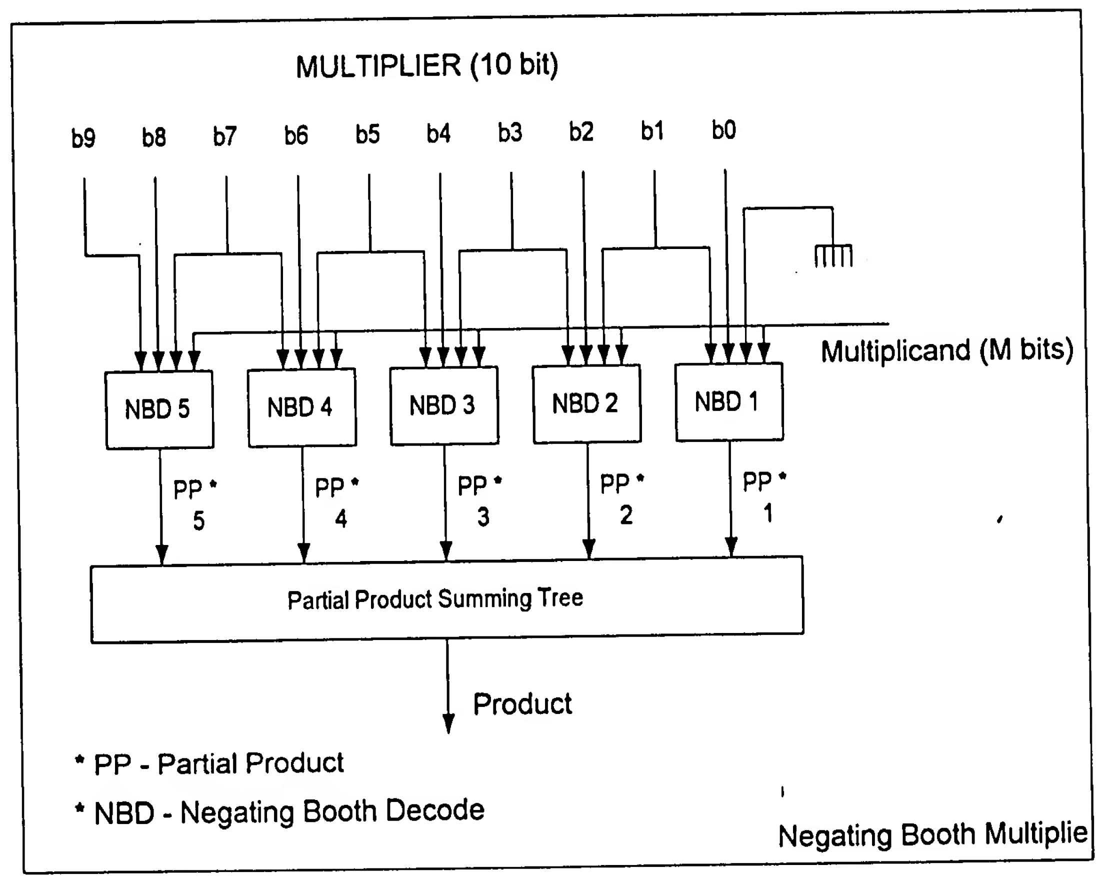
MULTIPLIER (10 bit)
b9
b8
b7
b6
b5
b4
b3
b2
b1
b0
Multiplicand (M bits)
NBD 5
NBD 4
NBD 3
NBD 2
NBD 1
PP * 5
PP * 4
PP * 3
PP * 2
PP * 1
Partial Product Summing Tree
Product
* PP - Partial Product
* NBD - Negating Booth Decode
Negating Booth Multiplie

FIG. 52

5300

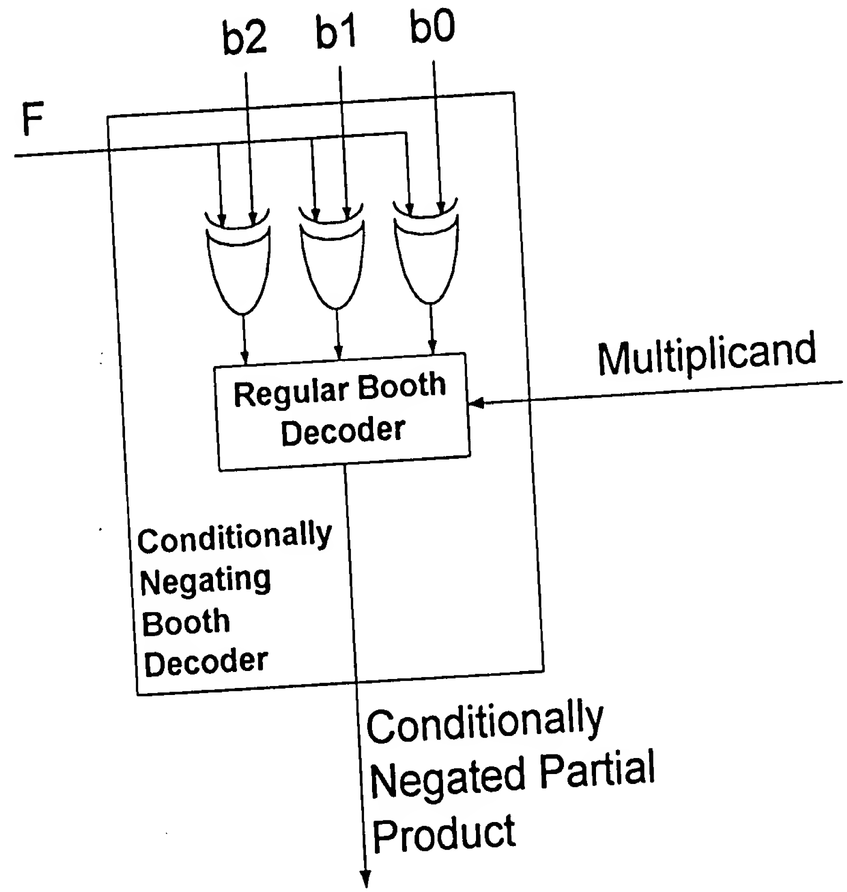
b2
b1
b0
F
Regular Booth Decoder
Multiplicand
Conditionally Negating Booth Decoder
Conditionally Negated Partial Product

FIG. 53

5400

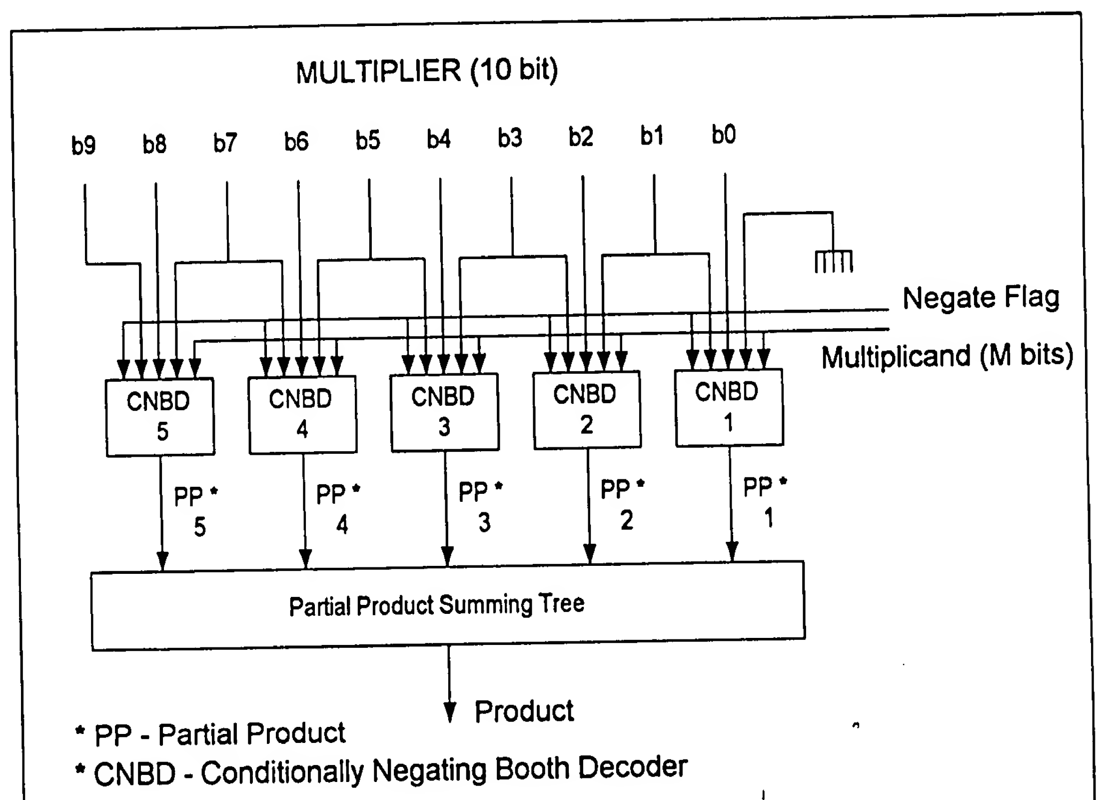

Conditionally Negating Booth Multiplier

FIG. 54

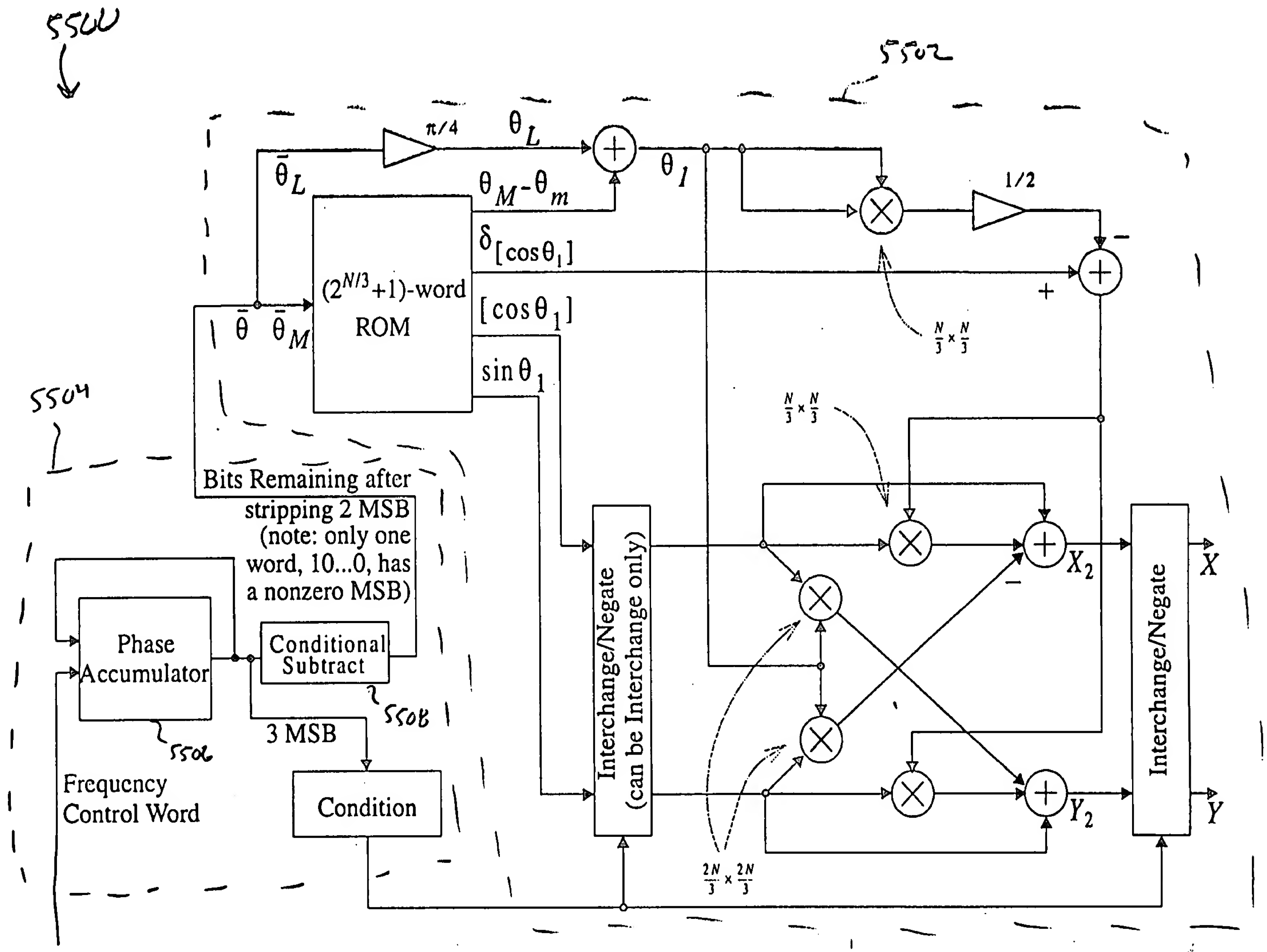

FIG. 55 Angle Rotator Configured as a Quadrature Direct Digital Synthesizer (QDDS).

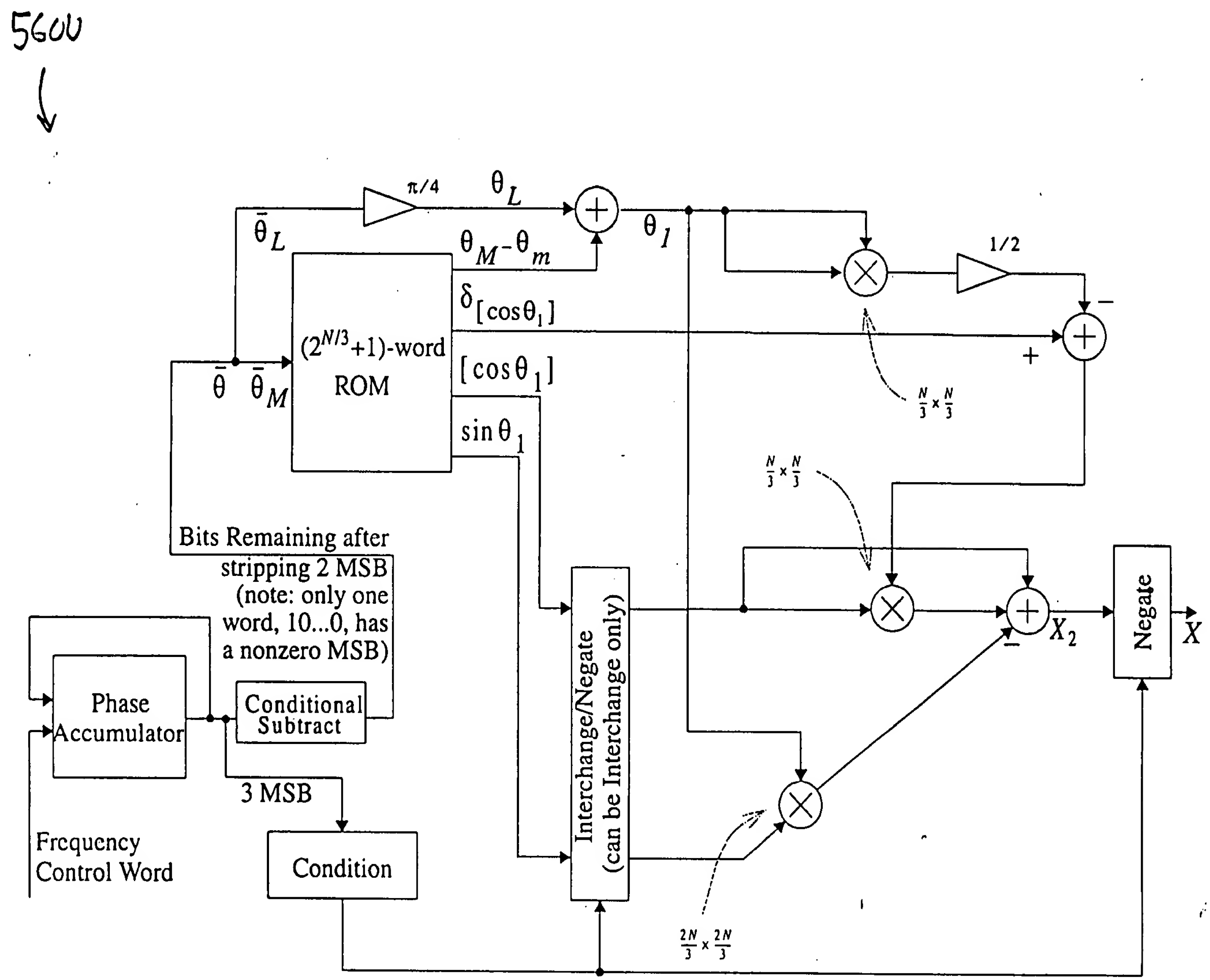

FIG. 56 Angle Rotator Configured as a "Cosine-only" Direct Digital Synthesizer (DDS) {from Fig 39}.

5700

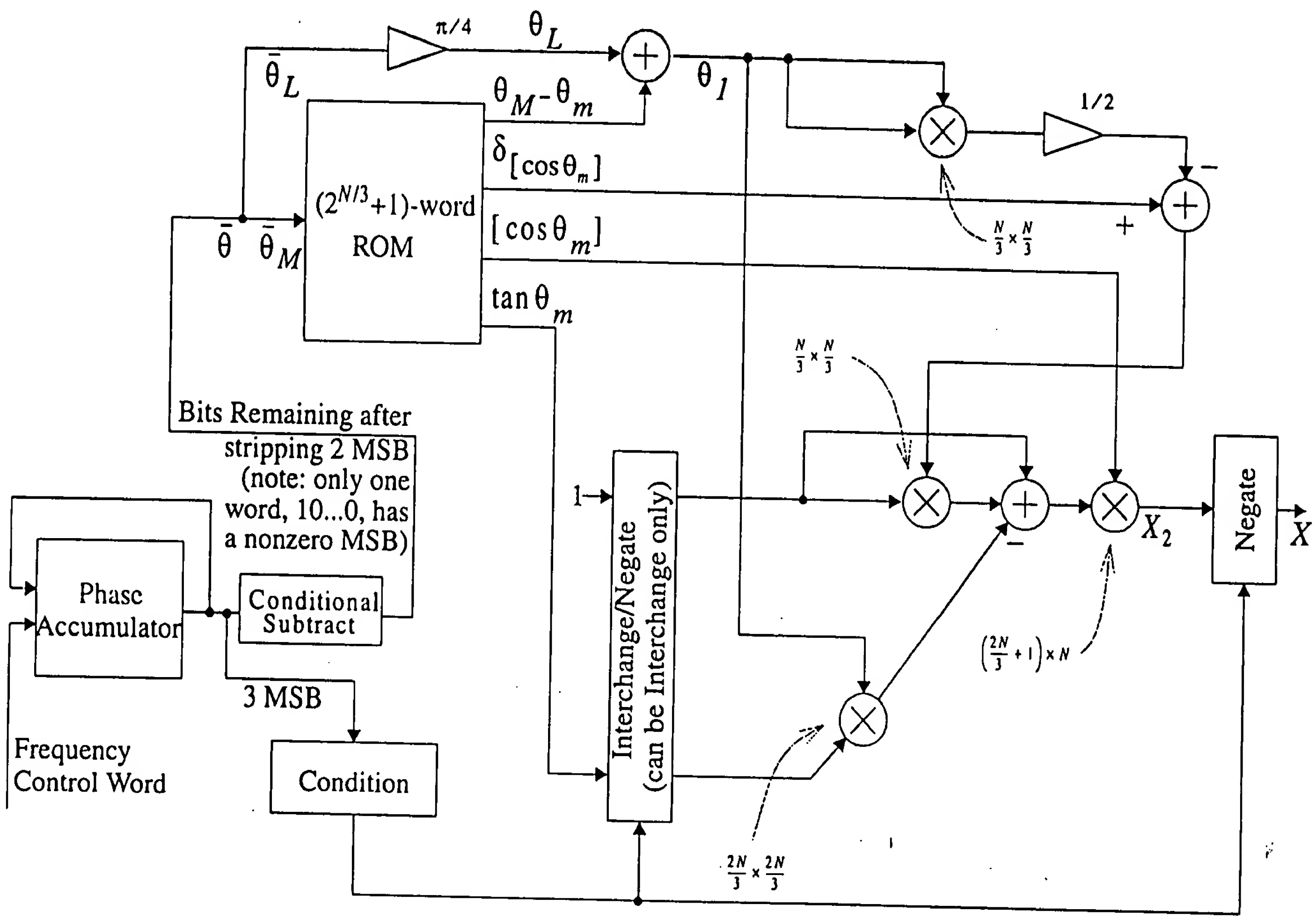

FIG. 57 Angle Rotator Configured as a "Cosine-only" Direct Digital Synthesizer (DDS) {from Fig. 44 .

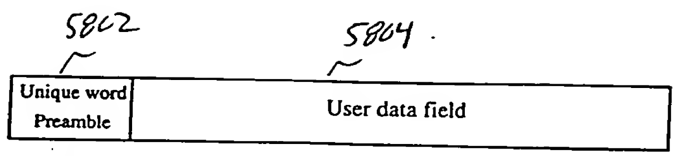

FIG. 58: Common packet format.

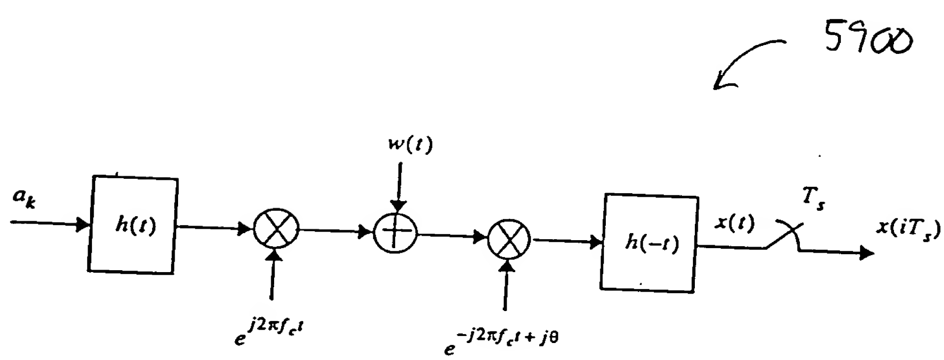

FIG. 59: The simplified system model.

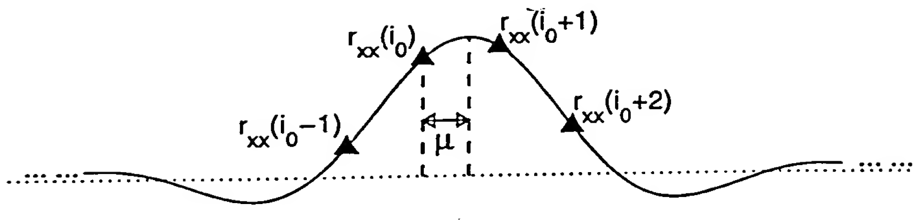

FIG. 60 Mean values of the preamble correlator output, for $\theta = 0$.

6100

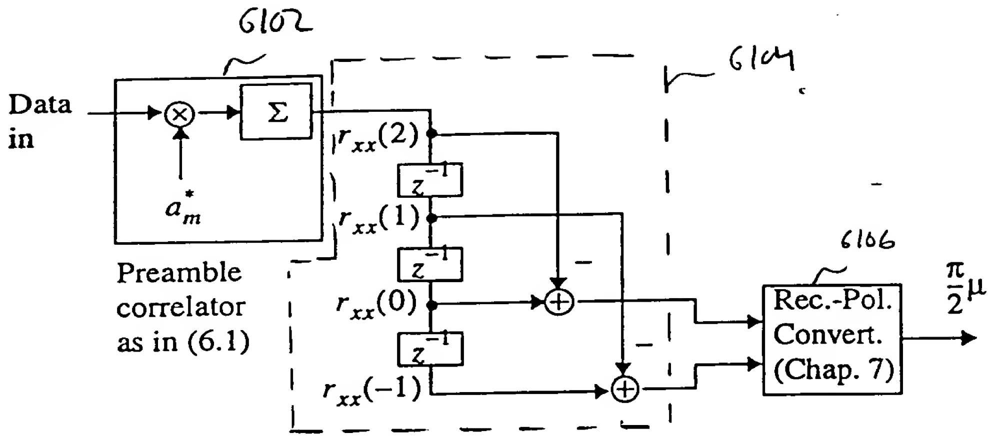

FIG. 61: Preliminary symbol-timing estimation structure.

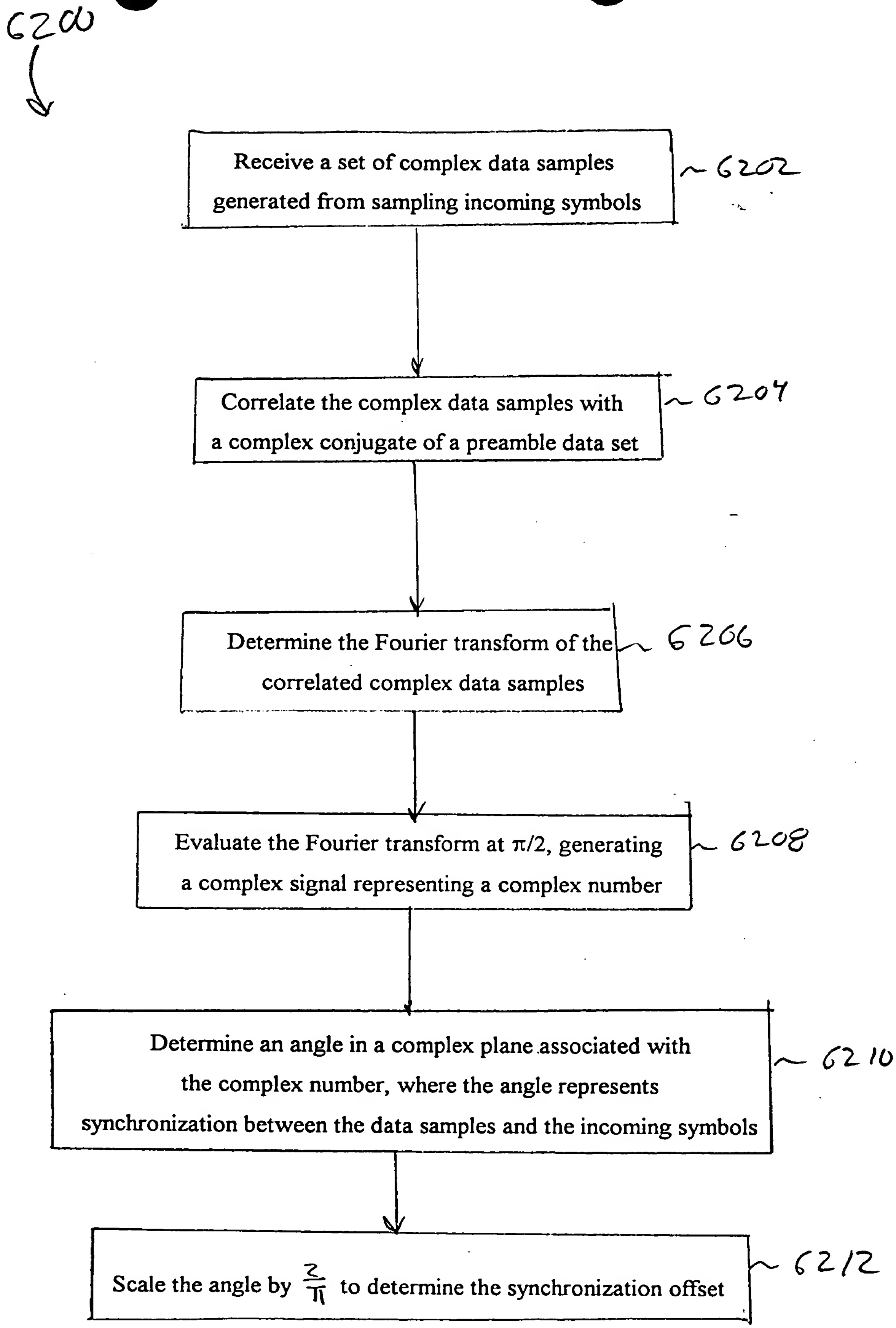
6200
Receive a set of complex data samples generated from sampling incoming symbols
6202
Correlate the complex data samples with a complex conjugate of a preamble data set
6204
Determine the Fourier transform of the correlated complex data samples
6206
Evaluate the Fourier transform at π/2, generating a complex signal representing a complex number
6208
Determine an angle in a complex plane associated with the complex number, where the angle represents synchronization between the data samples and the incoming symbols
6210
Scale the angle by 2/π to determine the synchronization offset
6212

FIG. 62

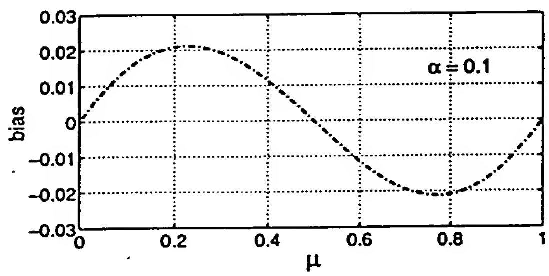

FIG. 63 Bias due to truncation.

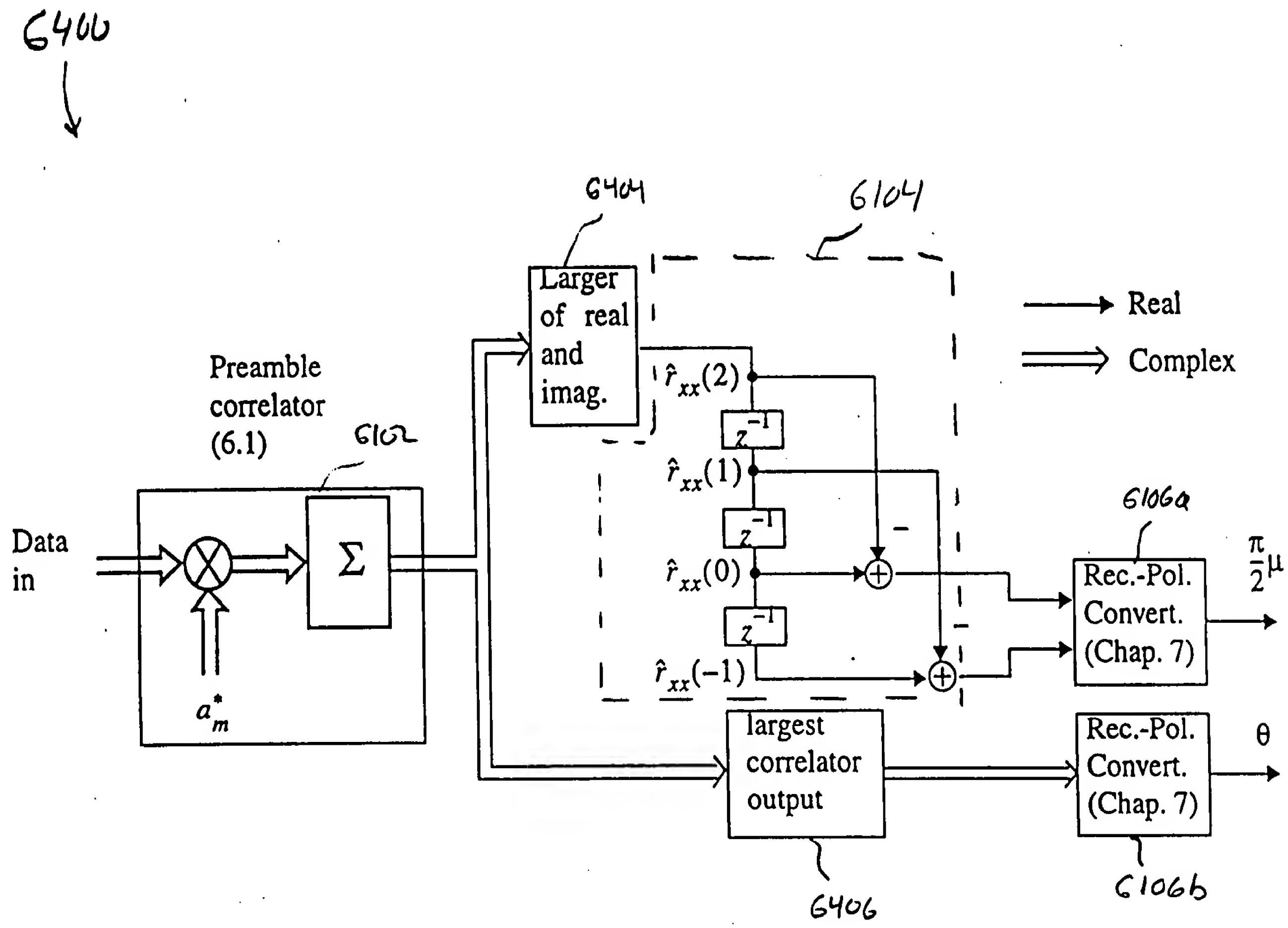

FIG. 64 Structure for carrier-phase and symbol timing recovery.

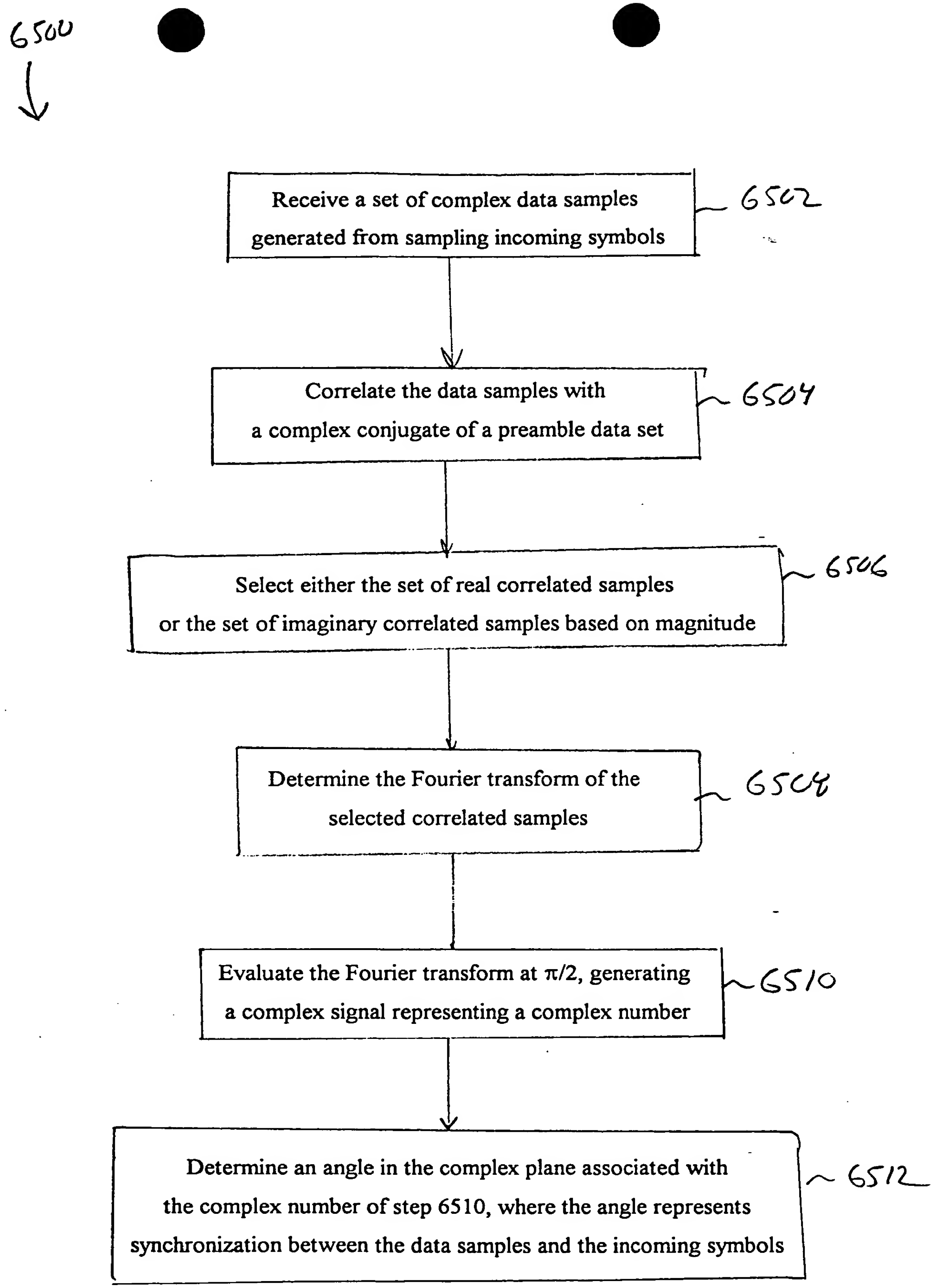
6500
Receive a set of complex data samples generated from sampling incoming symbols
6502
Correlate the data samples with a complex conjugate of a preamble data set
6504
Select either the set of real correlated samples or the set of imaginary correlated samples based on magnitude
6506
Determine the Fourier transform of the selected correlated samples
6508
Evaluate the Fourier transform at π/2, generating a complex signal representing a complex number
6510
Determine an angle in the complex plane associated with the complex number of step 6510, where the angle represents synchronization between the data samples and the incoming symbols
6512

FIG. 65A

6500 (cont.)

Scale the angle by π/2 to determine the synchronization offset 6514

Select the largest correlator complex output 6516

Determine an angle in the complex plane associated with the largest correlator complex output of step 6516, where the angle represents carrier phase offset θ 6518

FIG. 65B

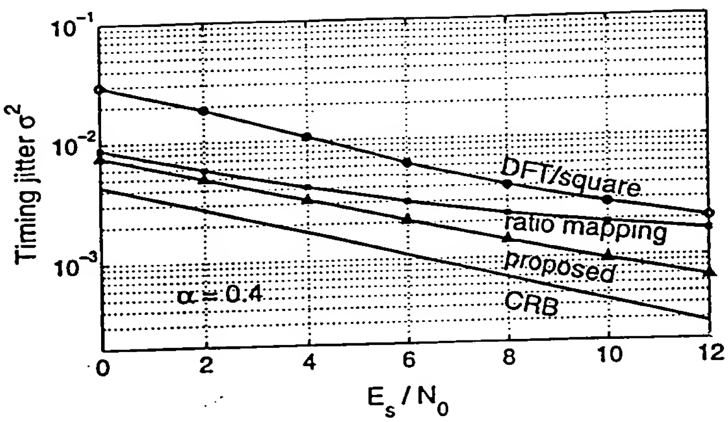

Figure 66: Timing jitter variance, $\alpha = 0.4$.

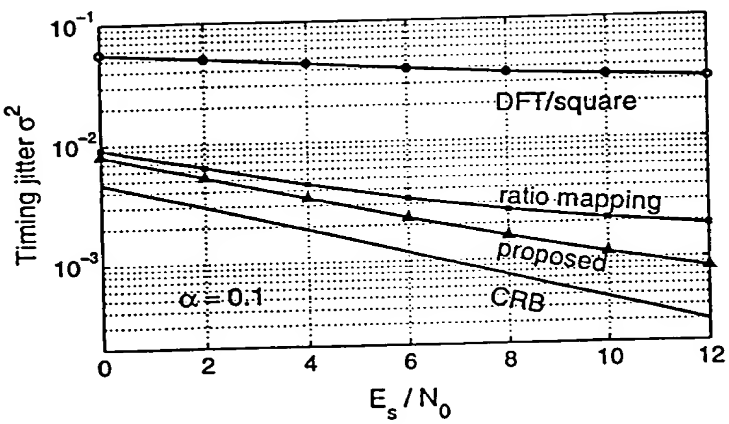

Figure 67: Timing jitter variance, $\alpha = 0.1$.

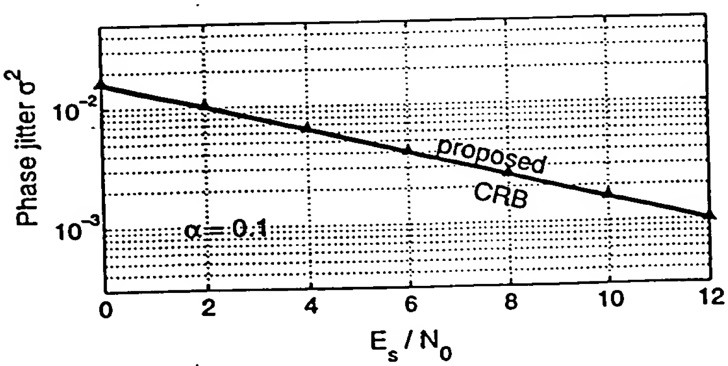

Figure 68: Phase jitter variance, $\alpha = 0.1$.

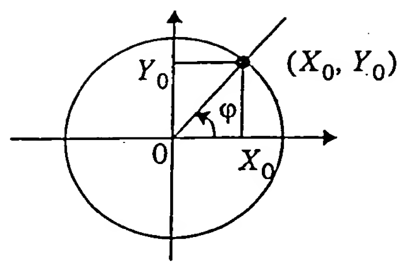

FIG. 69 Cartesian to polar conversion.

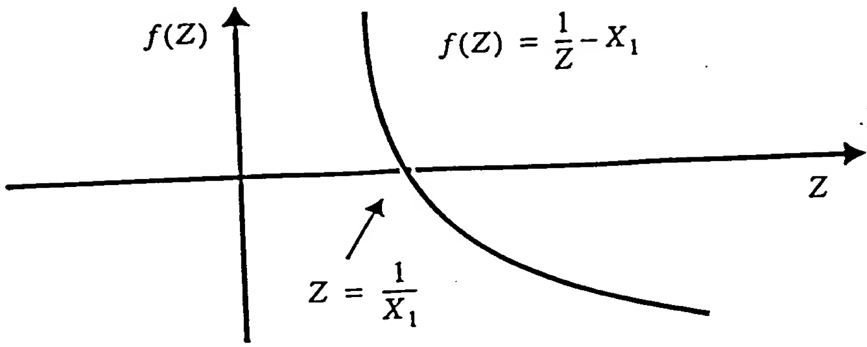

FIG. 70A: Using Newton-Raphson iteration to find $1/X_1$.

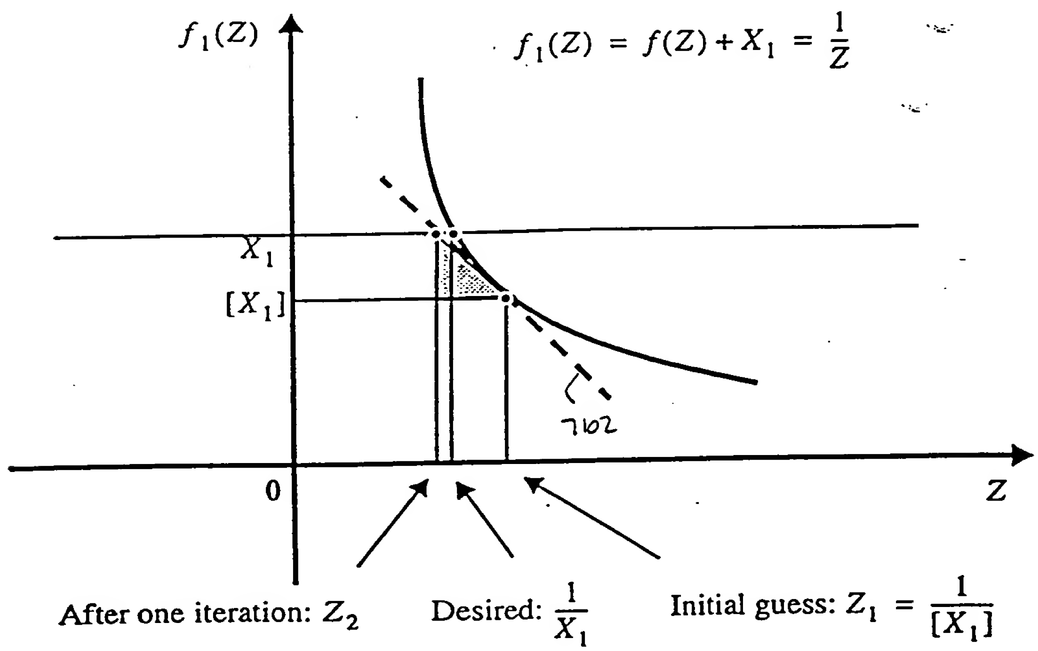

FIG. 70B: One Newton-Raphson iteration.

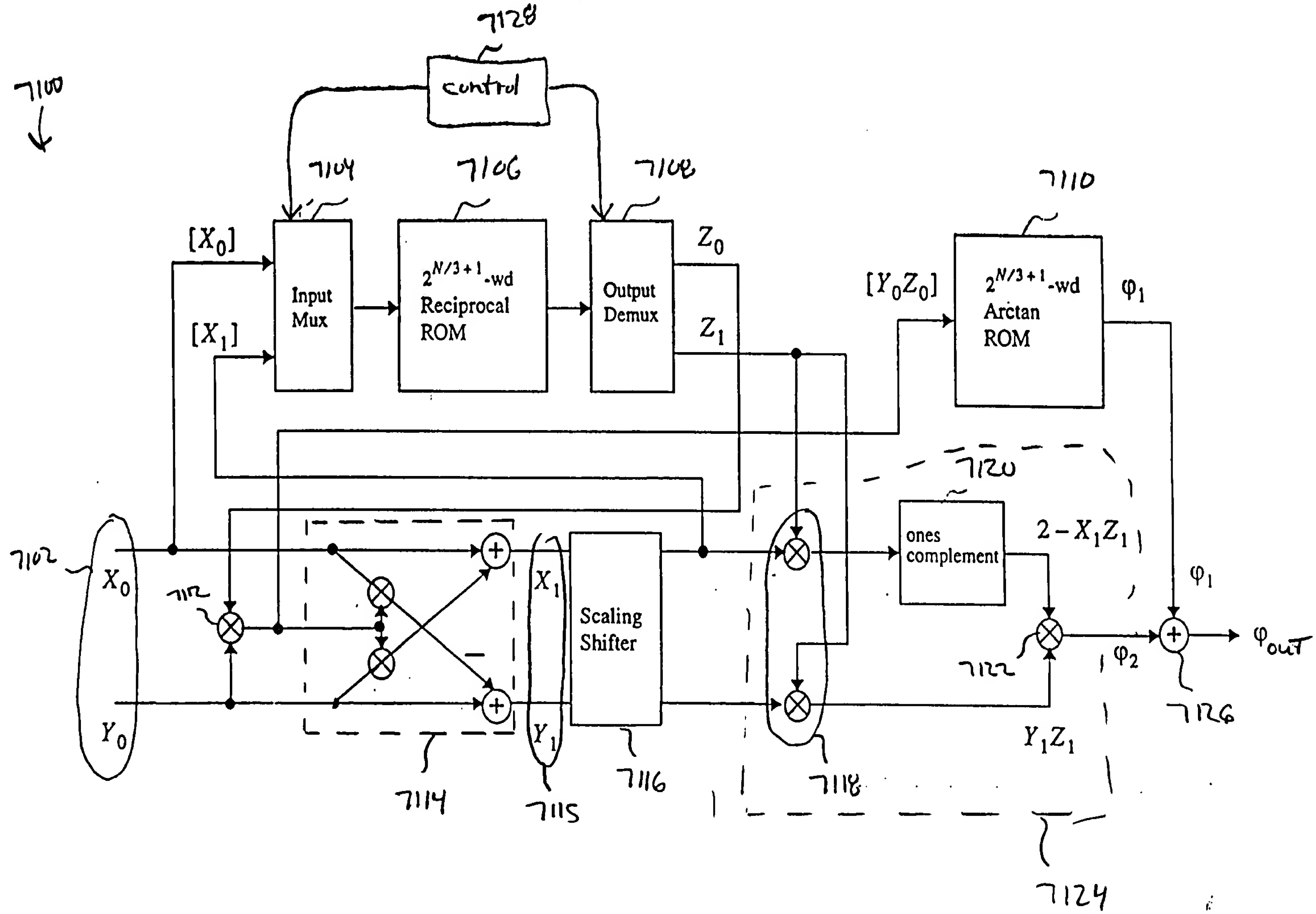
7100
7128
control
7104
7106
7108
7110
$[X_0]$
$[X_1]$
Input Mux
$2^{N/3+1}$-wd Reciprocal ROM
Output Demux
Z_0
Z_1
$[Y_0Z_0]$
$2^{N/3+1}$-wd Arctan ROM
φ_1
7120
ones complement
$2-X_1Z_1$
φ_1
φ_2
φ_{OUT}
7102
X_0
Y_0
7112
X_1
Y_1
Scaling Shifter
7122
7126
Y_1Z_1
7114
7115
7116
7118
7124

FIG. 71:

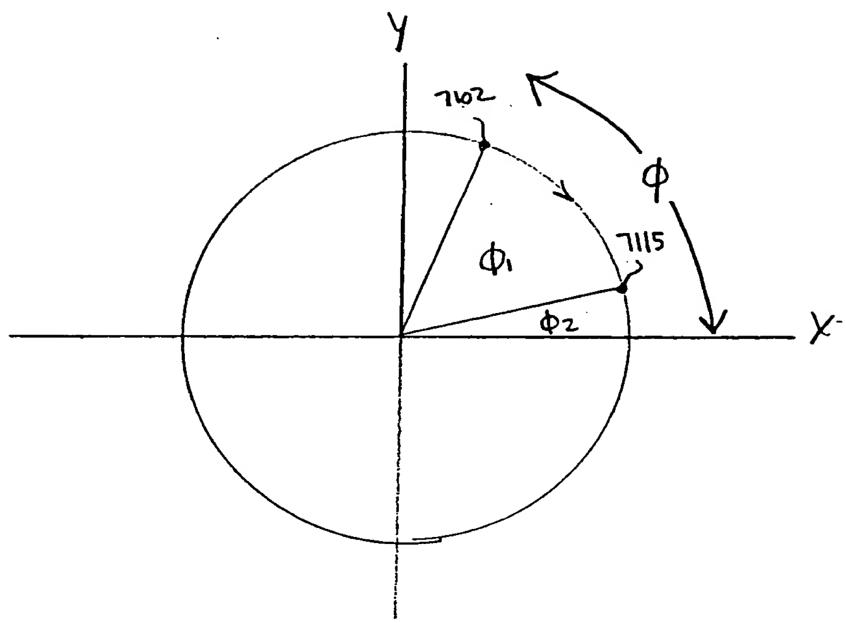

FIG. 72

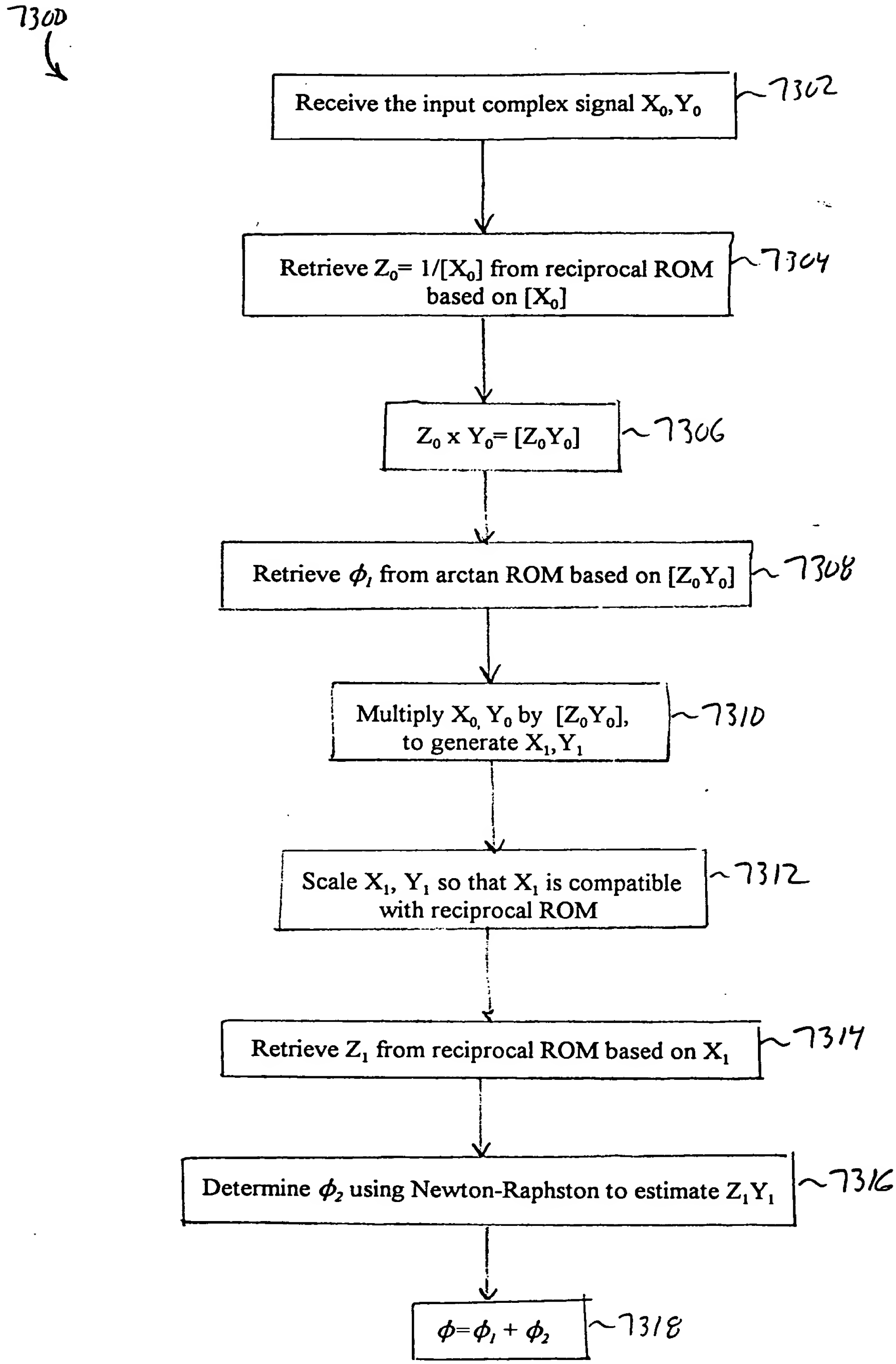
7300
Receive the input complex signal X_0, Y_0
7302
Retrieve $Z_0 = 1/[X_0]$ from reciprocal ROM based on $[X_0]$
7304
$Z_0 \times Y_0 = [Z_0 Y_0]$
7306
Retrieve ϕ_1 from arctan ROM based on $[Z_0 Y_0]$
7308
Multiply X_0, Y_0 by $[Z_0 Y_0]$, to generate X_1, Y_1
7310
Scale X_1, Y_1 so that X_1 is compatible with reciprocal ROM
7312
Retrieve Z_1 from reciprocal ROM based on X_1
7314
Determine ϕ_2 using Newton-Raphston to estimate $Z_1 Y_1$
7316
$\phi = \phi_1 + \phi_2$
7318

FIG. 73

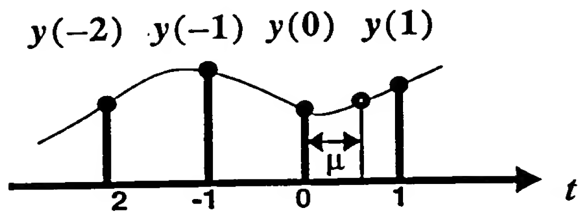

FIG. 74 Interpolation in a non-center interval.

FIG. 75A

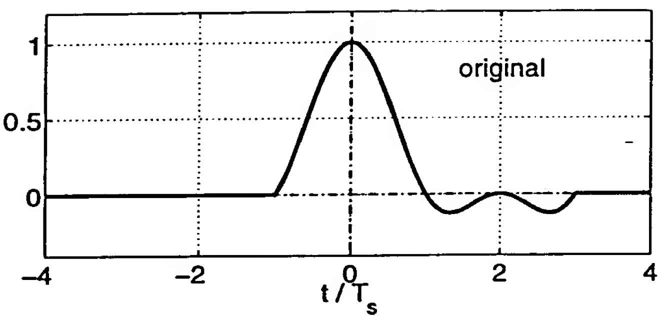

FIG 75B

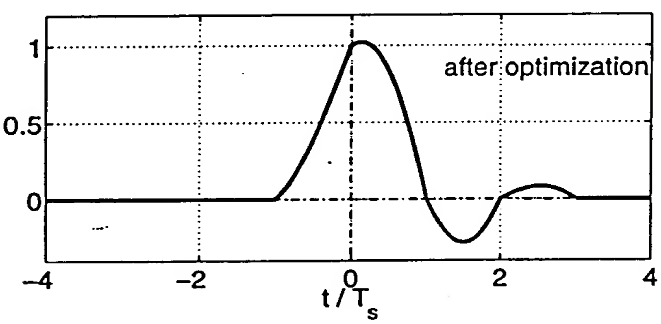

FIG. 75A-B: Impulse responses of the non-center-interval interpolation filter A before and B after optimization.

FIG. 76A

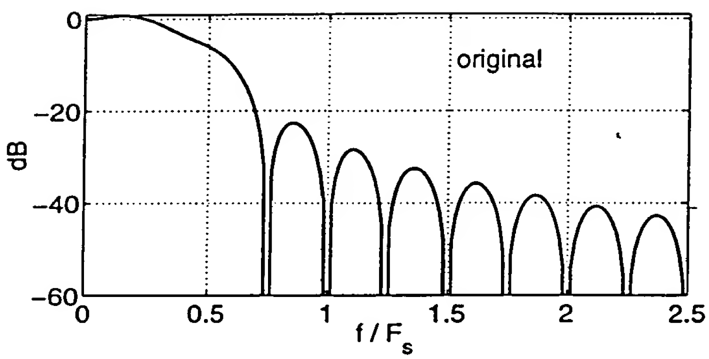

FIG. 76B

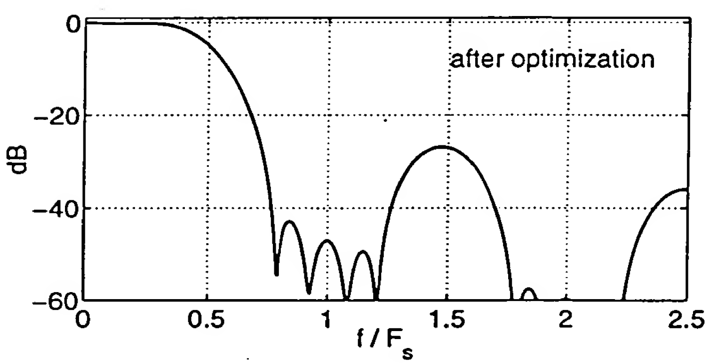

FIG. 76A-B: Frequency responses of the non-center-interval interpolator , before optimization and , after optimization.

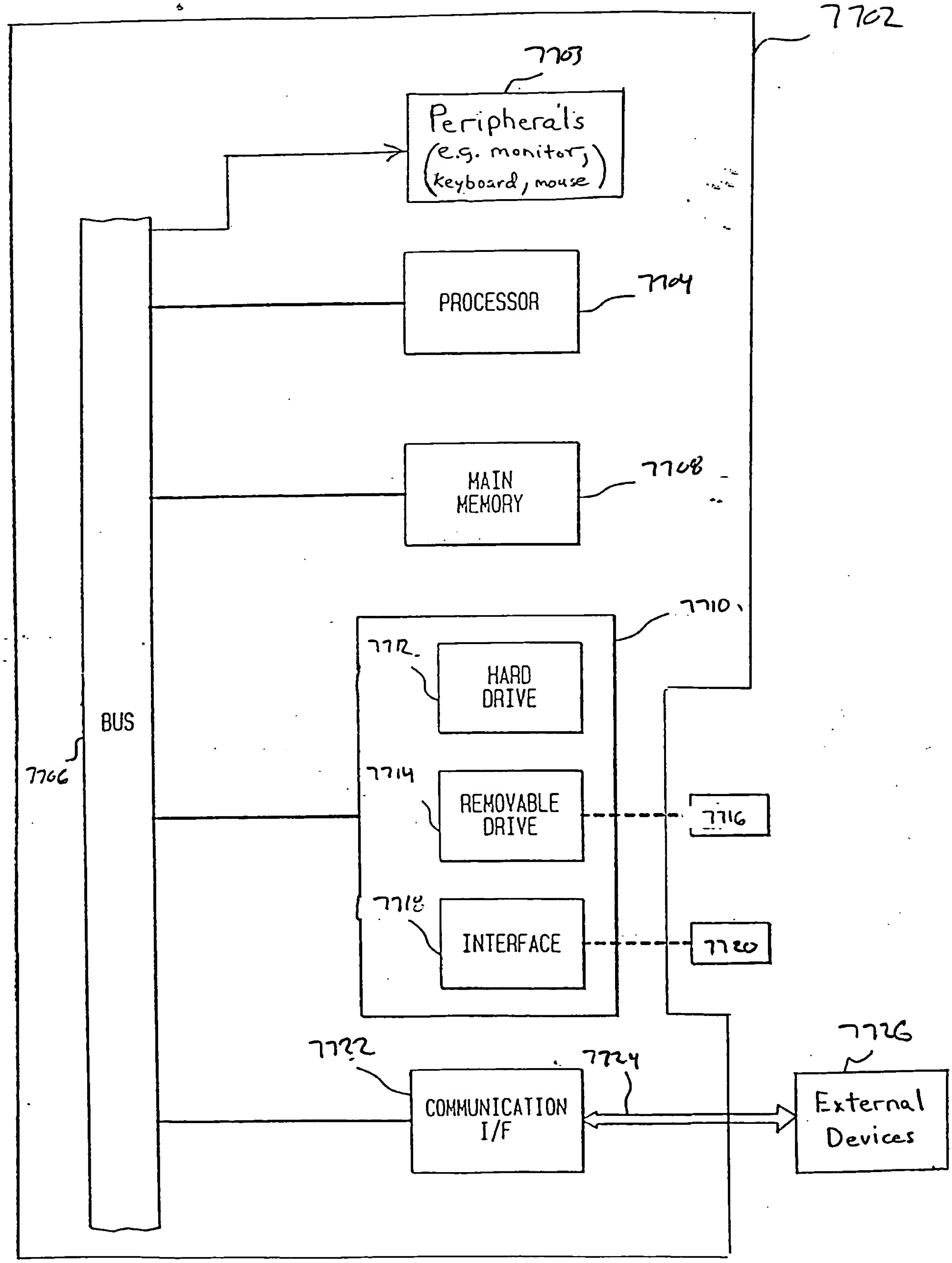

7702
7703
Peripherals (e.g. monitor, keyboard, mouse)
PROCESSOR
7704
MAIN MEMORY
7708
7710
7712
HARD DRIVE
7714
REMOVABLE DRIVE
7716
7718
INTERFACE
7720
BUS
7706
7722
7724
COMMUNICATION I/F
7726
External Devices

FIG. 77

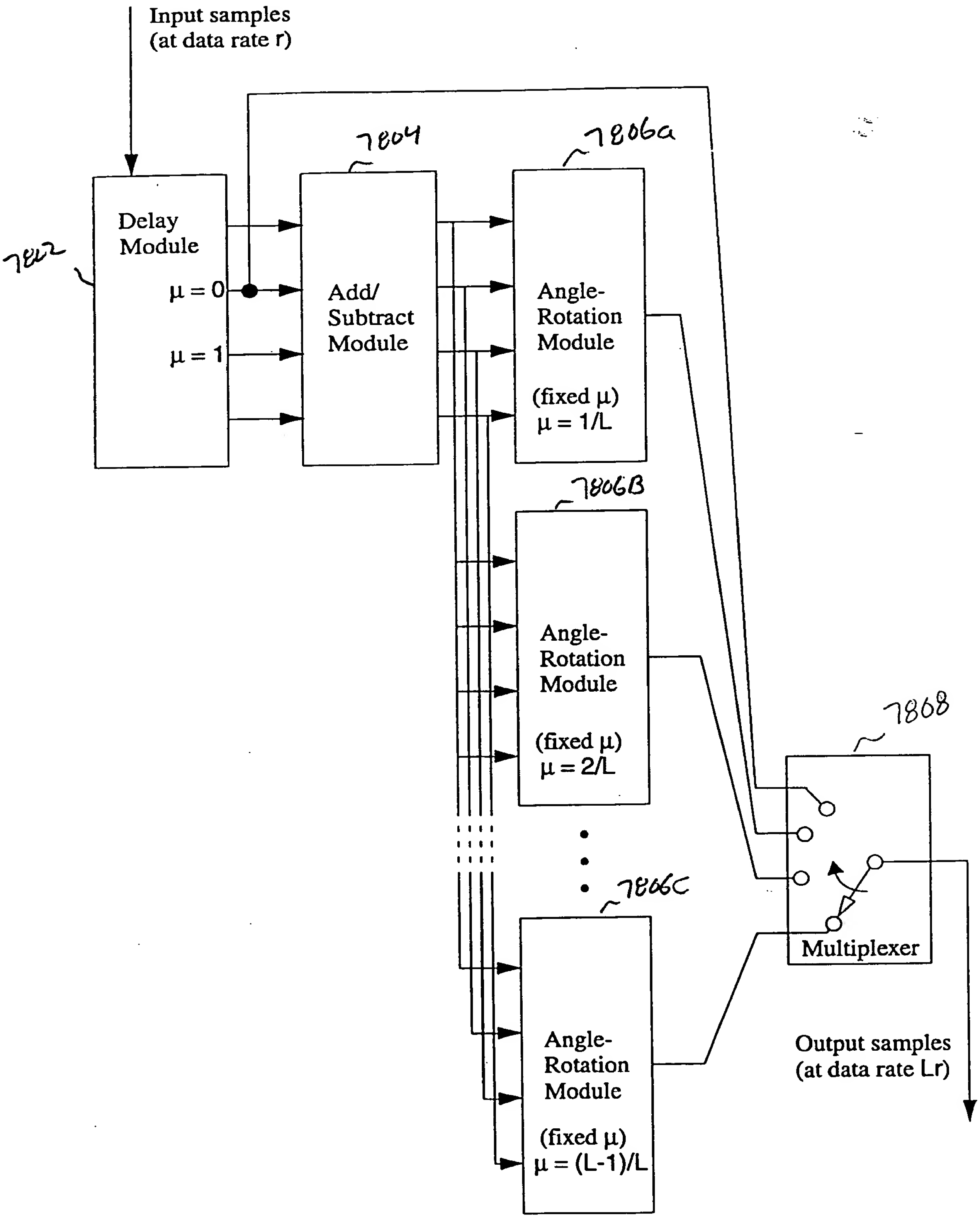

FIG. 78 Data Rate Expansion Circuit.